Radiative effect of clouds on tropospheric chemistry

in a global three-dimensional chemical transport model

Hongyu Liu[1], James H. Crawford[2], Robert B. Pierce[2], Peter Norris[3,4], Steven E. Platnick[3], Gao Chen[2], Jennifer A. Logan[5], Robert M. Yantosca[5], Mat J. Evans[5,6], Chieko Kittaka[7], Yan Feng[8], and Xuexi Tie[9]

[1]National Institute of Aerospace, Hampton, VA
[2]NASA Langley Research Center, Hampton, VA
[3]NASA Goddard Space Flight Center, Greenbelt, MD
[4]University of Maryland, Baltimore County, MD
[5]Harvard University, Cambridge, MA
[6]Now at University of Leeds, UK
[7]Science Applications International Corporation, Hampton, VA
[8]University of Michigan, Ann Arbor, MI
[9]National Center for Atmospheric Research, Boulder, CO

Short Title: Radiative effect of clouds on chemistry

Index Terms: 0365 Atmospheric Composition and Structure: Troposphere-composition and chemistry; 0360 Atmospheric Composition and Structure: Transmission and scattering of radiation; 3359 Meteorology and Atmospheric Dynamics: Radiative processes

Keywords: photolysis frequency, tropospheric ozone, hydroxyl radical, solar radiation, cloud optical depth, cloud overlap assumption

Submitted to Journal of Geophysical Research - Atmospheres, revised, January 2006.

Correspondence: Hongyu Liu
National Institute of Aerospace
100 Exploration Way
Hampton, VA 23666-6147
Tel: 609-452-6500 ext.6995; Fax: 609-987-5063
Tel: 757-325-6904; Fax: 757-325-6988 (after March 31, 2006)
Email: hyl@nianet.org

Abstract. Clouds exert an important influence on tropospheric photochemistry through modification of solar radiation that determines photolysis frequencies (J-values). We assess the radiative effect of clouds on photolysis frequencies and key oxidants in the troposphere with a global three-dimensional (3-D) chemical transport model (GEOS-CHEM) driven by assimilated meteorological observations from the Goddard Earth Observing System data assimilation system (GEOS DAS) at the NASA Global Modeling and Assimilation Office (GMAO). We focus on the year of 2001 with the GEOS-3 meteorological observations. Photolysis frequencies are calculated using the Fast-J radiative transfer algorithm. The GEOS-3 global cloud optical depth and cloud fraction are evaluated and generally consistent with the satellite retrieval products from the Moderate Resolution Imaging Spectroradiometer (MODIS) and the International Satellite Cloud Climatology Project (ISCCP). Results using the linear assumption, which assumes linear scaling of cloud optical depth with cloud fraction in a grid-box, show global mean OH concentrations generally increase by less than 6% due to the radiative effect of clouds. The OH distribution shows much larger changes (with maximum decrease of ~20% near the surface), reflecting the opposite effects of enhanced (weakened) photochemistry above (below) clouds. The global mean photolysis frequencies for $J[O^1D]$ and $J[NO_2]$ in the troposphere change by less than 5% due to clouds; global mean O_3 concentrations in the troposphere increase by less than 5%. This study shows tropical upper tropospheric O_3 to be less sensitive to the radiative effect of clouds than previously reported (~5% versus ~20-30%). These results emphasize that the dominant effect of clouds is to influence the vertical redistribution of the intensity of photochemical activity while global average effects remain modest, again contrasting with previous studies. Differing vertical distributions of clouds may explain part, but not majority, of these discrepancies between models. Using an approximate random overlap or a maximum-

random overlap scheme to take account of the effect of cloud overlap in the vertical reduces the impact of clouds on photochemistry, but does not significantly change our results with respect to the modest global average effect.

1. Introduction

Clouds play critical roles in influencing not only the earth's climate through modulation of the earth's energy and hydrological cycles but also tropospheric photochemistry through modification of solar radiation that determines photolysis frequencies [e.g., *Thompson*, 1984; *Crawford et al.*, 1999; *Yang and Levy*, 2004]. The uncertainty in radiative processes associated with clouds has been widely recognized as one of the key issues in current assessments of climate change [*Cess et al.*, 1996; *Houghton et al.*, 2001]. The radiative effect of clouds on tropospheric photochemistry and the associated uncertainty have been paid much less attention in the literature. A quantitative understanding of this effect is required for using global models to assess anthropogenic perturbations to the Earth system. We address here this issue with a global three-dimensional (3-D) chemical transport model or CTM (GEOS-CHEM) [*Bey et al.*, 2001a] driven by assimilated meteorological observations.

Clouds affect tropospheric chemistry in a variety of ways. They provide surfaces for heterogeneous chemistry to take place [*Jacob*, 2000]. Precipitating clouds scavenge soluble trace gases and aerosols from the troposphere [e.g., *Liu et al.*, 2001]. The vertical motions associated with clouds result in substantial convective transport of chemical species. In particular, deep convection can provide an important source of hydrogen oxide radicals in the upper troposphere, leading to enhanced production of ozone [*Prather and Jacob*, 1997]. Lightning associated with deep convective clouds is an important source of nitrogen oxides in the middle and upper troposphere [e.g., *Pickering et al.*, 1998]. Clouds also scatter and absorb incoming solar radiation, modifying the actinic flux and thus photolysis frequencies of key chemical species. The enhanced photolysis frequencies have been observed above and in the upper levels of clouds, while reduced frequencies were found below optically thick clouds and

absorbing aerosols [e.g., *Junkermann*, 1994; *Lefer et al.*, 2003]. Since photolytical processes are the sources of free radicals, clouds play an important role in determining the oxidative capacity of the troposphere [*Thompson et al.*, 1990].

In order to account for the spatial and temporal variability of photolysis frequencies under different atmospheric conditions, tropospheric chemistry models require photolysis schemes that are computationally efficient. Earlier CTMs often calculated photolysis frequencies offline and then tabulated them for interpolation during model integration for varying solar zenith angles [e.g., *Penner et al.*, 1991; *Brasseur et al.*, 1998]. As *Wild et al.* [2000] pointed out, however, pre-calculation does not allow interactive inclusion of the effects of the simulated ozone column or of highly variable cloud or aerosol loading, although using more detailed parameterizations or a correction factor during model integration may partly address the problem [*Berntsen and Isaksen*, 1997; *Landgraf and Crutzen*, 1998; *Feng et al.*, 2004]. A new scheme for calculating photolysis frequencies on-line (Fast-J) that is fast, flexible, and deals accurately with multiple scattering, was developed by *Wild et al.* [2000]. Fast-J has been incorporated into a number of CTMs [*Wild et al.*, 2000; *Shindell et al.*, 2001], including the GEOS-CHEM model [*Bey et al.*, 2001a] used in this study. Another efficient photolysis scheme (fast-TUV) using similar methodology and based on the Tropospheric Ultraviolet-Visible Model (TUV) was recently developed by *Tie et al.* [2003].

Several previous modeling studies have examined the radiative effect of clouds on photolysis frequencies and/or oxidants in the troposphere. *Tang et al.* [2003] used a 3-D regional CTM (STEM) coupled with the TUV model to study the influences of aerosols and clouds on photolysis frequencies and photochemical processes over the Asian-Pacific Rim during the TRACE-P period (February-April, 2001). Linear scaling of the cloud optical depth in a grid box

with cloud fraction (or uniform cloud distribution; referred to as LIN hereafter) was assumed. They found that clouds have a large impact on photolysis frequencies with $J[NO_2]$ decreased by 20% below clouds and enhanced by ~30% from 1km to 8km. Clouds were also found to reduce OH by 23% at <1km and increase OH by ~25% above 1km. *Mao et al.* [2003] conducted sensitivity experiments of clouds with a radiative transfer model and found that the impact of low and middle clouds on photolysis frequencies was stronger than high clouds by a factor of 2-3 due to large optical depths. *Tie et al.* [2003] suggested that the impact of clouds is probably unrealistically large when LIN is applied to calculate the photolysis frequencies in their global CTM (MOZART-2 coupled with fast-TUV).

One of the important issues or uncertainties when examining the radiative effect of clouds in models concerns how to represent the vertical coherence of clouds. A number of schemes have been introduced to address the effects of vertical subgrid variability of cloudiness on radiative transfer. The most commonly used schemes are the random overlap (RAN) and the maximum-random overlap (MRAN) assumptions [e.g., *Geleyn and Hollingsworth*, 1979; *Briegleb*, 1992; *Liang and Wang*, 1997; *Stubenrauch et al.*, 1997; *Collins*, 2001; *Stephens et al.*, 2004]. *Stephens et al.* [2004] presented an assessment of these and other different approaches for parameterizing the effects of cloud overlap on radiative transfer in a single radiation model. Photochemical models have just begun to take account of the effect of cloud overlap assumptions [*Tie et al.*, 2003; *Feng et al.*, 2004].

Tie et al. [2003] considered the subgrid vertical distribution of clouds by using MRAN in the calculation of photolysis frequencies in a global CTM. They found that with MRAN clouds increase global mean OH concentrations by about 20%, photolysis rates of $J[O^1D]$ and $J[NO_2]$ in the troposphere by about 12-13%, and tropospheric O_3 concentrations by 8%. It was suggested

that clouds have important impacts on tropospheric chemistry. They also argued that LIN tends to significantly overestimate backscattering above clouds and the overall impact on photochemistry in the troposphere. This argument was based on their calculation that showed the estimated global OH with LIN is about 50% higher than that with MRAN. *Feng et al.* [2004] were the first to systematically evaluate the effect of different cloud overlap assumptions (LIN, RAN and MRAN) on averaged photolysis frequencies and OH concentrations in a global photochemical model. Photolysis frequencies are increased in the upper tropical troposphere and decreased in the lower troposphere if LIN or RAN is followed rather than MRAN.

In this study, we apply GEOS-CHEM coupled with Fast-J to quantify the radiative effect of clouds on photolysis rates and key oxidants in the troposphere and to examine the effect of various cloud overlap assumptions. These are essentially the same issues investigated by *Tie et al.* [2003] and *Feng et al.* [2004]. Our results, however, contrast with those of *Tie et al.* [2003] in finding that the dominant effect of clouds is to influence the vertical redistribution of the intensity of photochemical activity while the global average effect remains modest. In particular, we will show that tropical upper tropospheric ozone concentrations in GEOS-CHEM are much less sensitive to the radiative effect of clouds than those in MOZART-2 as reported by *Tie et al.* [2003]. With online calculation of photolysis frequencies, we also improve over the study of *Feng et al.* [2004] with respect to the impact of different cloud overlap schemes.

The remainder of this paper is organized as follows. Section 2 will briefly describe the GEOS-CHEM model, the Fast-J algorithm, and the cloud overlap assumptions used. Section 3 will present the global distribution of cloud and its evaluation with satellite observations. One-dimensional test cases for offline calculation of photolysis frequencies using Fast-J are examined in section 4. The global impact of GEOS-3 clouds on photolysis frequencies under different

cloud overlap assumptions is assessed in section 5. The radiative effect of clouds on tropospheric key oxidants is examined in section 6, followed by discussion in section 7, and summary and conclusions in section 8.

2. Model and Methods

2.1. GEOS-CHEM

GEOS-CHEM is a global 3-D model of tropospheric O_3-NO_x-hydrocarbon chemistry coupled to aerosol chemistry. The model is driven by assimilated meteorological observations from the Goddard Earth Observing System (GEOS) of the NASA Global Modeling and Data Assimilation Office (GMAO). This study is based on GEOS-CHEM version 5.5 (see http://www-as.harvard.edu/chemistry/trop/geos) driven by 2000 and 2001 GEOS-3 meteorological data.

Bey et al. [2001a] presented a first description of the model as applied to simulation of tropospheric O_3-NO_x-hydrocarbon chemistry. The model was updated by *Martin et al.* [2002], and by *Park et al.* [2004] where aerosol (including sulfate-nitrate-ammonium, carbonaceous aerosols, sea salt, and mineral dust) chemistry is coupled with O_3-NO_x-hydrocarbon chemistry. The GEOS-3 data, including cloud fields, have 6-hour temporal resolution (3-hour resolution for surface fields and mixing depths), 1^o latitude by 1^o longitude horizontal resolution, and 48 sigma vertical levels extending up to 0.01 hPa. For computational efficiency, we degrade the horizontal resolution to 4^ox5^o and merge the 26 vertical levels above 85 hPa, retaining a total of 30. The midpoints of the lowest eight levels in the GEOS-3 data are at 10, 50, 100, 200, 350, 600, 850, and 1250 m above the surface for a column based at sea level. All simulations in this study were conducted for August 2000 - December 2001 using standard model output as initial conditions.

August-December 2000 was used for initialization and we analyze the model results for the year of 2001.

The model solves the chemical evolution of over 80 chemical species with a fast Gear solver and transports 31 chemical tracers. The model uses the advection scheme of *Lin and Rood* [1996]. The moist convective mixing scheme is that of *Allen et al.* [1996]. Wet deposition of soluble species includes scavenging in wet convective updrafts, and first-order rainout and washout from both convective and large-scale precipitation [*Liu et al.*, 2001; *Park et al.*, 2004]. The Synoz (synthetic O_3) scheme [*McLinden et al.*, 2000] is used as a flux upper boundary condition for O_3 in the stratosphere by imposing a global cross-tropopause flux of 475 Tg O_3 per year. We impose a uniform global CH_4 concentration of 1700 ppbv. Procedures for specifying emissions are described in *Bey et al.* [2001a]. This version of the model also includes an improved biomass burning emission inventory with seasonal variability constrained by satellite observations [*Duncan et al.*, 2003]. Lightning NO_x source is 6 Tg N yr^{-1} [*Martin et al.*, 2002].

A global evaluation of the GEOS-CHEM simulation of tropospheric O_3-NO_x-hydrocarbon chemistry was first presented by *Bey et al.* [2001a]. The model reproduces the climatological monthly mean O_3 concentrations from the ozonesonde observations to within usually 10 ppbv, and captures the phase of the seasonal cycle to within 1-2 months, with the seasonal amplitude underestimated at northern mid-latitudes. More specific evaluations of model results (using GEOS-1, GEOS1-STRAT, or GEOS-3) with O_3 observations in different regions of the world have been conducted for the Asian Pacific [*Bey et al.*, 2001b; *Liu et al.*, 2002, 2004], the Middle East [*Li et al.*, 2001], the United States [*Fiore et al.*, 2002ab, 2003ab], the North Atlantic [*Li et al.*, 2002ab], and the tropics [*Martin et al.*, 2002; *Chandra et al.*, 2003]. A detailed description and global evaluation of the model simulation for CO is presented by B.N.

Duncan et al. (Model study of the variability and trends of carbon monoxide (1988-1997): 1. Model formulation, evaluation, and sensitivity, submitted to Journal of Geophysical Research, 2004). The low CO and high OH in the old version of the model [*Bey et al.*, 2001a] has been improved in the current version by the consideration of minor sources from oxidation of previously neglected volatile organic compounds.

2.2. Photolysis calculation

Photolysis frequencies in GEOS-CHEM are calculated with the Fast-J radiative transfer algorithm of *Wild et al.* [2000], which uses a seven-wavelength quadrature scheme and accounts accurately for Rayleigh scattering as well as Mie scattering by aerosols and clouds. Fast-J achieves the accuracy of the calculated photolysis frequencies generally to within 3% [*Wild et al.*, 2000] and compares well with other photolysis schemes [*Olson et al.*, 1997].

A total of 52 photolysis reactions are included in GEOS-CHEM (The GEOS-CHEM Chemical Mechanism version 5-05-03, by Arlene Fiore and Daniel Jacob, Harvard University, June 2003; electronic copy of this document available at http://www-as.harvard.edu/chemistry/trop/geos/geos_mech.html). Photolysis calculations are performed every hour and thus diurnal variations are represented. Vertically resolved cloud optical depths and cloud fractions are taken from the GEOS-3 meteorological archive with 6-hour resolution. Monthly mean surface albedos are those of *Herman and Celarier* [1997]. This version of GEOS-CHEM uses climatological ozone concentrations as a function of latitude, altitude, and month to calculate the absorption of UV radiation by ozone. We find by sensitivity experiments that using tropospheric ozone concentrations from the model simulation (versus climatology) has little effect on our results presented in this paper.

2.3. Cloud Overlap Assumptions

Following *Feng et al.* [2004], we examine in this study three assumptions about the vertical subgrid variability of clouds including the linear scheme, the approximate random overlap scheme, and the maximum-random overlap scheme and evaluate their effects on photolysis frequencies and key oxidants. These schemes are discussed in details in *Feng et al.* [2004] and *Tie et al.* [2003] and are briefly summarized here as follows.

Linear Assumption (LIN). The most commonly used assumption in current CTMs is that clouds cover an entire horizontal grid with a cloud optical depth averaged over the clear and cloudy areas in each layer, which assumes that the actinic flux is linearly proportional to cloud optical depth [*Feng et al.*, 2004]. That is, the grid average cloud optical depth $\tau_c' = \tau_c \cdot f$, where τ_c is the cloud optical depth in the cloudy portion of the grid and f is the cloud fraction in each layer. This approach may introduce a significant bias because of the nonlinear relationship between photolysis frequencies and cloud optical depth.

Approximate Random Overlap (RAN). The random overlap scheme assumes that clouds in vertical layers are independent of each other and randomly overlapped. A detailed implementation of this scheme therefore requires extensive computations [*Feng et al.*, 2004]. *Briegleb* [1992] designed a formulation for cloud optical depth, i.e., $\tau_c' = \tau_c \cdot f^{3/2}$. *Briegleb* [1992] showed that this formulation yields a reasonable approximation to a detailed random overlap calculation for the heating rate. As *Feng et al.* [2004] demonstrated, for large cloud fractions, the scaling of cloud optical depth by cloud fraction to the 3/2 power is a good approximation to the exact random overlap calculation; for small cloud fraction, there are large errors. On a global scale cloud fraction is typically 60-70% (see section 3) so that one would expect the approximation is often a good one. This method has been widely used as an

approximation for the exact random overlap in global CTMs [e.g., *Brasseur et al.*, 1998], and is also adopted in this study (hereafter referred to as RAN).

Maximum-Random Overlap (MRAN). The maximum-random overlap scheme assumes that clouds in adjacent layers are maximally overlapped to form a cloud block and that blocks of clouds separated by clear layers are randomly overlapped [*Geleyn and Hollingsworth*, 1979]. A vertical profile of fractional cloudiness is converted into a series of column configurations with corresponding fractions (**Figure 1**). Any individual layer has either full or zero cloud cover. Radiative transfer calculation is conducted for each column configuration. Photolysis frequencies are then the average of all column radiation transfer calculations weighted by the column area fraction in each configuration. *Feng et al.* [2004] applied a version of MRAN [*Collins*, 2001] to study the effect of cloud overlap in their photochemical model. *Tie et al.* [2003] used a similar version of MRAN [*Stubenrauch et al.*, 1997] in their study of the radiative effect of clouds on photolysis rates and tropospheric oxidants. The major difference between the two versions of MRAN is that the latter assumes that within a cloud block the cloud fraction is equal to the maximum cloud fraction within those cloud layers and the water content in each cloud layer within the block is adjusted to conserve the total water content. The resulting number of configurations is significantly smaller for the latter than for the former. We find that the different assumptions about the overlap within a cloud block have less than 2-5% effect on monthly, zonal, and daily- mean photolysis rates. At a specific location, the vertically integrated photolysis rates can change by up to 8%. If not otherwise explicitly stated, we refer MRAN in the following discussions to the *Stubenrauch et al.* [1997] approach as used by *Tie et al.* [2003] that requires much less computing time.

3. Global Cloud Distribution and Evaluation With Satellite Observations

Cloud optical depth and cloud fraction are critical parameters needed to describe the radiative effect of clouds on tropospheric photochemistry. Fast-J requires as input the grid-scale cloud optical depth in vertical model layers. Model estimates of cloudiness and its vertical variability, however, have large uncertainties. We evaluate in this section the GEOS-3 cloud optical depth and cloud fraction with satellite retrieval products from the Moderate Resolution Imaging Spectroradiometer (MODIS, on Terra) [*Platnick et al.*, 2003] and the International Satellite Cloud Climatology Project (ISCCP) [*Rossow et al.*, 1996; *Rossow and Schiffer*, 1999].

The occurrence of clouds in GEOS-3 is empirically diagnosed based on grid-scale relative humidity and subgrid-scale convection (L. Takacs, personal communication, 2004). The cloud optical properties are empirically prescribed to obtain a reasonable simulation of top-of-the-atmosphere longwave and shortwave cloud forcing. For large-scale clouds, cloud optical depth is empirically assigned values proportional to the diagnosed large-scale liquid water. For convective clouds, cloud optical depth is prescribed as 16 per 100mb. A temperature-dependence is used to distinguish between water and ice clouds.

We show in **Figure 2** the global distribution of GEOS-3 monthly mean (grid-scale) cloud optical depths as compared to MODIS (MOD08_M3, level-3 monthly global product at 1^{o}x1^{o} resolution) and ISCCP (D2, 280km equal-area grid) retrievals for March 2001 when frequent cyclogenesis occurred in the Northern Hemisphere. Zonal mean plots for March, June, October, and December of 2001 are shown in **Figure 3**. The MODIS and ISCCP values are the scalar product of the cloud optical depth retrievals and their respective cloud fractions; thus, they represent average conditions accounting for both cloudy and clear conditions. This is necessary for a consistent comparison with model monthly mean optical depths. Using ISCCP 3-hourly

monthly mean cloud retrievals sampled at the Terra MODIS local equatorial crossing time (approximately 10:30am) has little effect on our results reported here. Both MODIS and ISCCP cloud optical depths reveal the maxima associated with tropical convection, extratropical cyclones in the Northern Hemisphere, and the marine stratiform clouds in the Southern Hemisphere (SH, ~50-60^{o}S). GEOS-3 shows the same features in cloud optical depths but tends to overestimate the values at ~50-60^{o}S as well as in the tropics. At northern high latitudes, GEOS-3 cloud optical depths do not show values as high as those from MODIS and ISCCP retrievals; the latter is presumably due to uncertainties associated with snow or ice cover in the satellite retrievals for these regions. GEOS-3 appears to capture the day-to-day variability in cloud optical depth associated with synoptic-scale frontally induced cloudiness in the Asian Pacific region during spring (not shown). Similar plots are constructed for monthly mean cloud fraction. GEOS-3 cloud fraction agrees, overall, with MODIS and ISCCP products, but tends to be somewhat lower at mid-latitudes (**Figure 4**).

While the MODIS and ISCCP monthly mean cloud optical depths presented in **Figures 2** and **3** are comparable in magnitude, note that it was first necessary to make some adjustments to the cloud optical depths reported by these two projects in order to make them directly comparable. This is because ISCCP values are based on radiative non-linearly averaged values of individual pixels while the MODIS values used were based on linear averages. This difference in averaging has led to previous reports of large differences (a factor of 2-3) between MODIS and ISCCP monthly mean cloud optical depths (R. Pinker et al., First use of MODIS data to cross-calibrate with GEWEX/SRB data sets, Global Energy and Water Cycle Experiment (GEWEX) NEWS, Vol. 13, No.4, November 2003). While the cloud optical depths reported in the ISCCP D2 dataset are averaged values of individual pixels with non-linear weights that preserve the

average cloud albedo, linear averages of individual pixel values of optical depth proportional to cloud water content are stored in the ISCCP D2 dataset as water path [*Rossow et al.*, 1996]. Thus to be consistent with the linearly averaged MODIS optical depths, we have used linearly averaged cloud optical depth derived from the ISCCP water path data.

The above evaluations of GEOS-3 cloud optical depth and cloud fraction provide a quantitative estimate of errors in these fields, which are used in the radiative transfer calculations. One caveat, however, is that the range of visible optical depths that can be measured by satellites is typically ~0.5-100, limited by cloud detection limits at the lower end and lack of further sensitivity at the upper end [*Hartmann et al.*, 1999]. On the other hand, there is at present a lack of information about the global climatology of the vertical distribution of cloud amount and optical depth, preventing a reliable evaluation of cloud vertical distributions in GEOS-3.

4. Effect of Cloud on Photolysis Rates: Test Cases

4.1. Effect of Cloud Overlap

We use the one-dimensional test cases designed by *Feng et al.* [2004] to evaluate Fast-J photolysis frequencies calculation and the effect of different cloud overlap assumptions. As *Feng et al.* [2004] showed, the effect of cloud overlap is sensitive to cloud fraction as well as to solar zenith angle. We illustrate this for J[O^1D] in **Figures 5 and 6** for 0° and 60° solar zenith angles, respectively. Atmospheric conditions are based on those of 45°N summer. Total ozone column is 330DU. Surface albedo is 0.1. We assume here clouds are fully scattering and do not include aerosols. In **Figures 5ab** and **6ab**, clouds with a large mean optical depth of 54 are placed between 2-3km and 3-4km with either small cloud fraction (0.1 and 0.2, respectively) or large cloud fraction (0.8 and 0.9, respectively). In **Figure 5c** and **6c**, clouds with a small mean optical depth of 6 are placed between 2-3km and 3-4km with cloud fractions of 0.2 and 0.3, respectively.

Relative to clear-sky conditions, the presence of the optically thick cloud leads to enhancement of J[O^1D] above the cloud (as well as in the upper part of the cloud) and reduction below the cloud. In the case of small cloud fraction, this effect of clouds on J[O^1D] is substantially larger in LIN and RAN than in MRAN because clouds extend to the entire layer in the former two schemes, leading to more reflection of solar radiation from the cloud below and less radiation penetrating through the cloud (**Figure 5a**). RAN gives J[O^1D] that are closer to those in MRAN because of the scaling of cloud optical depth by cloud fraction to the 3/2 power in RAN. In the case of large cloud fraction, the differences in both the enhancement of J[O^1D] above the cloud and the reduction below the cloud are relatively small (**Figure 5b**). Because global cloud coverage is about 60-70%, this may have an important implication for the global effects of cloud overlap treatment. In case of small cloud optical depth (**Figure5c**), the cloud column optical depth is larger in MRAN than in RAN because of line-up of clouds in adjacent layers [*Feng et al.*, 2004]. MRAN therefore gives larger enhancements (reductions) of J[O^1D] than RAN does above (below) the cloud. LIN continues to give the largest enhancement above the cloud. At the large solar zenith angles of 60^o (**Figure 6**), the reduction of J[O^1D] below the cloud in RAN and LIN is enhanced compared to MRAN, in particular for small cloud fraction. With small cloud fraction, MRAN gives the largest J[O^1D] below the cloud (**Figure 6c**), contrasting with the smallest values at zero solar zenith angle (**Figure 5c**).

To summarize, our calculation of J[O^1D] for clear sky and different overlap assumptions using the Fast-J algorithm generally reproduces the features revealed by the calculation of *Feng et al.* [2004] using the TUV model, lending confidence to the implementation of cloud overlap assumptions in this study. Relative to LIN and RAN, MRAN decreases the radiative impact of

clouds on photolysis frequencies for optically thick clouds, but increases the impact below optically thin clouds at small solar zenith angles.

4.2. Sensitivity to Vertical Cloud Distributions and Cloud Water Contents

We assess the sensitivity of the impact of clouds on photolysis rates to different vertical cloud distributions and cloud water contents (or optical depths) by using the test cases designed by *Tie et al.* [2003]. Three different vertical cloud distributions are assumed: (1) a single cloud layer between 0-3km (low cloud case); (2) a single cloud layer between 9-11km (high cloud case); (3) multi-layer clouds between 0-3km and 9-11km (multi-layer cloud case). Atmospheric conditions are based on those of tropical regions (13°N). The cloud liquid water content is 0.1 g/m^3. The cloud optical depth is then obtained by [*Slingo and Schrecker*, 1982]:

$$\tau = \beta\, dz, \quad \beta = 3\, LWC / (2\, r_e),$$

where τ is the cloud optical depth, β is the extinction coefficient (m^{-1}), LWC is the cloud liquid water content (g/m^3), dz is the thickness of cloudy layer (m), and r_e is the effective radius for cloud liquid water droplets (typically ~10μm). Following *Tie et al.* [2003], we use the MRAN cloud overlap scheme, a cloud fraction of 50%, and r_e of 20μm [Tie et al., 2006]. Surface albedo is set to 0.1. Total ozone column is 258.6DU. We assume the cloud single scattering albedo (SSA) to be 1.0 (full scattering). It is noted that *Tie et al.* [2003, 2006] used an unrealistic value of 0.99 for SSA in their 1-D test cases while using a more typical value of 0.999 in their global model simulations. **Figure 7** shows the Fast-J calculated $J[O^1D]$ under both clear and cloudy conditions for three different vertical cloud distributions and at four solar zenith angles (0°, 30°, 60°, and 75°). **Table 1** shows the sensitivity of $J[O^1D]$ (and $J[NO_2]$) to the cloud optical depth by changing cloud liquid water content by ±50%.

With overhead sun, in the case of low cloud layer, $J[O^1D]$ is enhanced above and throughout much of the cloud, with a maximum near the top of the cloud (**Figure 7a**). The total enhancement averaged over the whole troposphere is about 19% (**Table 1**). For the high cloud case, $J[O^1D]$ increases above the cloud and throughout much of the cloud, and decreases below the cloud. On average, $J[O^1D]$ increases only 1.5% in the troposphere. For the multi-layer cloud case, a larger $J[O^1D]$ enhancement is seen above the high cloud layer due to radiation reflected from the low cloud layer; the latter also explains the enhancements between the two cloud layers. $J[O^1D]$ decreases near the surface. Overall change in $J[O^1D]$ is about 18% in the troposphere. Compared to the results reported by *Tie et al.* [2003] with the TUV model, our calculation indicates significantly larger increases (smaller decreases) in $J[O^1D]$ above (below) the cloud, reflecting mainly our assumption of full scattering cloud (SSA=1.0). If we use the same SSA (i.e., 0.99) as in *Tie et al.* [2003], the percentage changes in $J[O^1D]$ as indicated above would be 8.9%, -9.7%, and -3.6%, respectively, and they would be much closer to those reported by Tie et al. [2003] (12.7%, -5.7%, and -9.3%, respectively).

As *Tie et al.* [2003] found, the impact of clouds on photolysis is very sensitive to the vertical location of clouds as well as the cloud water content (**Table 1**). Interestingly, this impact is more sensitive to the vertical location of clouds than to the cloud water content. An important implication, as mentioned earlier, is that having a reasonable vertical distribution of cloudiness is essential for taking account of the radiative effect of clouds. On the other hand, we can see from **Table 1** that with increasing solar zenith angles, the enhancement above the low cloud decreases and the reduction below the high cloud increases, due to larger path lengths.

5. Global Impact of Clouds on Photolysis Frequencies

In this section, we assess the global impact of clouds on photolysis frequencies by coupling Fast-J with GEOS-CHEM, including the effect of cloud overlap. We focus on photolysis frequencies J[O^1D] and J[NO_2] which are most important for determining OH and O_3 concentrations.

Figures 8ab show the percentage changes in monthly daily-mean J[O^1D] due to the radiative effect of clouds as simulated by GEOS-CHEM with (a) LIN and (b) RAN for June 2001. Also shown in Figure 8a is the latitude-altitude cross-section of zonal mean GEOS-3 cloud optical depth per kilometer. In the tropics, J[O^1D] is enhanced by up to ~20% above the clouds, and reduced by up to ~10-20% below; it reflects the backscattering (attenuation) of solar radiation above (below) the deep convective clouds. Similar effects are also seen above and below the low level clouds at NH and SH midlatitudes. Above the clouds, NH sees larger enhancements (~10%) than SH does (~5%) in spite of smaller column cloud optical depth in the model (**Figure 3**); this is because of smaller solar zenith angles in NH at this time of the year (see **Table 1**). Near the surface, J[O^1D] are reduced by ~20-30% at all latitudes. As expected, using RAN leads to a smaller impact of clouds on J[O^1D] because more solar radiation is able to penetrate through the clouds (**Figures 8ab**). Nevertheless, LIN and RAN give similar patterns in terms of the regions of J[O^1D] enhancements and reductions due to the radiative impact of clouds.

As *Feng et al.* [2004] pointed out, observational studies have not been able to distinguish whether RAN or MRAN is preferred. We choose to use MRAN as the reference because previous studies found that cloud overlap might best be modeled as a combination of random and maximum overlap [*Hogan and Illingworth*, 2000]. **Figures 8cd** show the percentage differences in daily-mean J[O^1D] between LIN and MRAN, RAN and MRAN, respectively, as simulated by

GEOS-CHEM. LIN overestimates reflection of solar radiation above the clouds in particular in the tropics (up to 10%) and overestimates the reduction near the surface by ~10% (**Figure 8c**). The differences between RAN and MRAN are generally ~2% and not more than ~5% anywhere (**Figure 8d**). The relatively larger differences (~5%) in the tropical middle and upper troposphere reflect an overestimate of actinic fluxes in RAN relative to MRAN, within deep convective clouds (**Figure 8d**) which typically have large optical depth and small cloud fraction (see **Figure 5**). Nevertheless, the computationally cheap RAN is overall a good approximation to the more expensive MRAN in terms of the calculated daily mean photolysis rates.

Similar plots are shown in **Figure 9** for J[NO_2]. The impact of clouds on J[NO_2] is comparable or larger than that on J[O^1D] (**Figure 9ab**). The major absorption by NO_2 occurs at longer wavelengths (near 380nm) than does the absorption by O_3; the former is less dependent on Rayleigh scattering [*Jacob et al.*, 1989; *Feng et al.*, 2004]. As a result, J[NO_2] is more sensitive to the presence of clouds than J[O^1D], as we can see from **Figures 8a and 9a**. At southern polar regions, J[NO_2] and J[O^1D] artificially change in opposite directions due to zonal and monthly averaging. This may also partly reflect the low accuracy of Fast-J at large solar zenith angles, an aspect that is improved in the updated Fast-J algorithm, the so-called Fast-JX. Compared to MRAN, LIN overestimates J[NO_2] above the clouds (up to ~10% in the tropics) and underestimates J[NO_2] below the clouds (up to ~10-20% near the surface) (**Figure 9c**). J[NO_2] differences between RAN and MRAN are less than ~2% except at southern polar regions with large solar zenith angles (**Figure 9d**).

6. Radiative Effect of Clouds on Key Oxidants

Cloud perturbations to photolysis frequencies affect tropospheric chemistry and, in particular key oxidants in the troposphere. We examine in this section the radiative effect of clouds on global OH and tropospheric O_3 budget, including the effect of cloud overlap. The radiative effect of clouds is represented by subtraction of the clear-sky simulation from the cloudy-sky simulation.

Global Mean Effect. Shown in **Table 2** are the percentage changes in the global tropospheric mean concentrations of key oxidants and global mean photolysis frequencies due to the radiative effect of clouds in June and December 2001, following Table 4 of *Tie et al.* [2003]. Our calculated global mean changes in OH, O_3, NO_x, HO_2, CH_2O, and CO are generally less than 6%, independent of the cloud overlap schemes used. The significantly larger changes in OH during December is mainly due to large cloud optical depths associated with the SH marine stratus in GEOS-3. This effect is probably an overestimate because GEOS-3 significantly overestimates these cloud optical depths (**Figure 3**). For other months, GEOS-3 gives cloud optical depths that are much closer to satellite retrievals (**Figure 3**). As we will show below, the fact that global mean effect remains modest in our model reflects an offsetting effect of above-cloud enhancements and below-cloud reductions. The same can be said for our calculated global changes in photolysis frequencies (section 5). The lifetime of methylchloroform (CH_3CCl_3, MCF) or CH_4 is a proxy for the global mean OH concentrations [*Spivakovsky et al.*, 1990]. We calculate the MCF lifetime as the ratio of the total burden of atmospheric MCF to the tropospheric loss rate against oxidation by OH [*Spivakovsky et al.*, 2000]. Annual mean lifetime of MCF (CH_4) for 2001 is 6.5 (11) years under clear-sky condition and changes by less than 6% under cloudy-sky condition using any of the cloud overlap schemes (**Table 2**). Interestingly, we find that the MCF (CH_4) lifetime may increase even if global mean OH concentrations increase.

This reflects the fact that the MCF (CH_4) lifetime is more sensitive to the OH concentrations in the lower troposphere (versus the middle and upper troposphere) because of the temperature-dependency of the MCF-OH (CH_4-OH) reaction constant. Our global MCF lifetime is within the range of previous estimates from observations (5-7 years) [*Spivakovsky et al.*, 2000; *Prinn et al.*, 2001].

Zonal Mean Effect. Figures 10ab show the percentage changes in monthly daily-mean OH due to the radiative effect of clouds as simulated by GEOS-CHEM with (a) LIN and (b) RAN for June 2001. In the tropics, OH is enhanced by up to ~5-10% above the deep convective clouds, and reduced by ~5-20% below, reflecting the backscattering (attenuation) of solar radiation above (below) the tropical convective clouds (**Figure 10a**). At NH midlatitudes, OH is enhanced by ~5-10% above the low level clouds; at SH subtropics, OH are enhanced by ~5%; at SH high-latitudes, the impact of clouds on OH does not show consistent patterns. Near the surface, OH decreases by ~-20% due to clouds. Using RAN rather than LIN reduces the impact of clouds on OH (**Figures 10ab**). Compared to MRAN, LIN underestimates OH by up to ~10% near the surface and overestimates OH by 5-10% above the low level clouds at NH midlatitudes and above the tropical clouds (**Figure 10c**). RAN gives OH concentrations that are close (within 5%) to those given by MRAN (not shown).

Figure 11a shows the percentage changes in monthly zonal mean O_3 due to the radiative effect of clouds (MRAN) in June 2001. The maximum impact on O_3 (~5%) is seen in the tropical upper troposphere with less than a few percent impact elsewhere. Contrasting with OH enhancements above clouds and reductions below clouds, O_3 enhancements are found in most of the troposphere, partly reflecting the short lifetime of OH (seconds) and relatively long lifetime of O_3 in the troposphere (days to a few weeks). The lower troposphere in the tropics and SH are

overall a regime of net O_3 loss due to low NO_x environments (not shown). We find that the presence of tropical deep convective clouds suppresses this net O_3 loss, thus increasing O_3 concentrations in this part of the troposphere. The maximum positive percentage changes (up to ~20-30%) in surface O_3 occur in the tropics (not shown), but large relative changes are usually associated with low ozone, resulting in small relative changes in zonal mean concentrations.

Figure 11b shows the percentage changes in monthly zonal mean CO due to the radiative effect of clouds (MRAN) in June 2001. Cloud overlap has little effect. The overall impact of clouds on CO is not significant, although NH (SH) tends to see positive (negative) changes. The small changes in CO may be due to the fact that loss of CO by OH is partly compensated by CO production from hydrocarbons. The positive (negative) changes in NH (SH) reflect the fact that CO sources are dominated by direct emissions in continental source regions in NH but by OH oxidation of hydrocarbons in SH.

Comparison with previous modeling. We compare here our model calculations with those of *Tie et al.* [2003]. There are some similarities. Both this study and that of *Tie et al.* [2003] found O_3 enhancements in most of the troposphere due to the radiative effect of clouds, but the latter indicated much larger enhancements of O_3 in the tropics with a maximum impact of ~20-30% in the upper troposphere (see their Figure 14). When LIN or RAN rather than MRAN is used in our model, neither do we see significantly larger impact on O_3. It appears that the sensitivities of O_3 to clouds in the two models, as they now stand, are quite different. Both studies found that using LIN and MRAN schemes have important effects on the calculation of the cloud effects, consistent with the study of *Feng et al.* [2004].

There are more discrepancies between the two model calculations. Also shown in **Table 2** are the MOZART-2 simulated percentage changes in the global tropospheric mean

concentrations of key oxidants and global mean photolysis frequencies due to the radiative effect of clouds, as reported by *Tie et al.* [2003, 2006]. The small changes in global means found in this study are in distinct contrast with the large percentage changes (except for NO_x) found in the MOZART-2 model [*Tie et al.*, 2003], in particular for OH (**Table 2**). *Tie et al.* [2003] reported a very similar CH_4 lifetime (11.4 years) under clear-sky condition but significantly different CH_4 lifetimes of ~5-6 years (LIN) and ~8-9 years (MRAN) under cloudy-sky conditions. Such dramatic changes in CH_4 lifetime (-18% - -46%) due to the presence of clouds or the use of different cloud overlap schemes are not seen in our model. There are some factors that may contribute to all these differences. First, we use mass weighted method to calculate the global mean changes in tropospheric chemical species, while those reported by *Tie et al.* [2003] are based on the volume mixing ratios averaged over each grid-box below 200mb (X. Tie, personal communication, 2004). The non-mass weighted method tends to give global mean concentrations erroneously weighted toward the middle and upper troposphere. Even if we calculate global mean changes in the same way as *Tie et al.* [2003] did, we do not find large percentage changes, only reflecting the offsetting effect of above-cloud enhancements and below-cloud reductions in our model. Second, the cloud vertical distributions in this study appear significantly different than those of *Tie et al.* [2003]. The MOZART-2 model uses on-line calculated cloud distribution with a high temporal-resolution (20 minutes time interval). As pointed out by *Tie et al.* [2003], MOZART-2 tends to underestimate high cloud water in the tropics (see their Figure 8) where our model has more high cloud water (by a factor of 2-3). Both models have low cloud water of similar magnitude, including in the tropics (not shown). Relative to our model, MOZART-2 may therefore overestimate the reflection of solar radiation from tropical low clouds. However, our sensitivity experiments suggest that different cloud vertical distributions cannot explain the

major discrepancies between the two model calculations (Liu et al., Sensitivity of tropospheric chemistry simulations to cloud vertical distributions and optical properties, manuscript in preparation for J. Geophys. Res., 2006; hereafter referred to as Liu et al., manuscript in preparation, 2006). At present, to compare the two studies in a systematic way is beyond the scope of this study.

7. Discussion

It is well established that tropospheric O_3 is an important greenhouse gas, in particular in the upper troposphere. Because cloud optical properties may change due to anthropogenic influences through aerosol-cloud interactions, the sensitivity of tropospheric O_3 is an important issue for assessment of anthropogenic perturbations to the climate. The reason for the different sensitivities of tropical upper tropospheric O_3 to clouds in GEOS-CHEM (this work) and MOZART-2 [*Tie et al.*, 2003] is not immediately clear. It appears that global distributions of clouds are similar in the two models, except in the tropics where the optical depth due to high clouds tends to be underestimated in MOZART-2 [*Tie et al.*, 2003]. We conducted a sensitivity simulation using GEOS-CHEM where the GEOS-3 clouds in the tropical middle and upper troposphere were removed. The results do not indicate a larger effect of clouds on O_3 either. It is also difficult to see how the different sensitivities might result from differences in the chemical mechanisms used in the two models. The global budget analysis of tropospheric O_3 in MOZART-2 suggests that its tropospheric chemistry is not significantly more active than that of other global models [*Horowitz et al.*, 2003]. We argue that a ~20-30% increase in tropical upper tropospheric O_3 solely due to the radiative effect of clouds is too large.

Cloud treatments and diagnostics are still the major uncertainty in climate models, as reflected by the discrepancies in the cloud optical and physical properties from various meteorological archives. These cloud fields may affect the simulation of the tropospheric chemistry system. For instance, the meteorological fields driving the GEOS-CHEM model include a series of archives from GEOS DAS, i.e., GEOS-1, GEOS1-STRAT, GEOS-3 (this study), and GEOS-4. The global average cloud optical depths in GEOS-1 and GEOS1-STRAT appear to be a factor of 4-5 smaller than those in GEOS-3 (not shown). Cloud optical depths in GEOS-4 seem too low in the tropics when compared to GEOS-3 as well as MODIS and ISCCP satellite retrieval products, reflecting the optically much thinner clouds in the tropical middle and upper troposphere in GEOS-4 (not shown). The differences between the sensitivity simulation mentioned above (where the clouds in the tropical middle and upper troposphere were removed) and the standard simulation give us a sense of the impact of GEOS-3 and GEOS-4 cloud optical depth differences on the simulation of tropospheric chemistry. It suggests that using GEOS-4 cloud optical depths may overestimate OH concentrations by about 10-20% in most of the tropical troposphere (**Figure 12**), if LIN is used. Indeed, a recent GEOS-CHEM full chemistry simulation driven by GEOS-4 showed significantly higher global OH concentrations than earlier simulations driven by GEOS-3 (Jennifer Logan, personal communication, 2004). We will document in a separate paper the sensitivity of tropospheric chemistry simulations to cloud vertical distributions and optical properties (Liu et al., manuscript in preparation, 2006). We suggest that the radiative effect of clouds on the simulation of tropospheric chemistry be assessed in the Global Modeling Initiative (GMI) framework [*Douglass et al.*, 1999] where the cloud fields from various meteorological archives can be utilized.

With respect to the effect of cloud overlap on photochemistry, we improve over the study of *Feng et al.* [2004] in at least two aspects. First, we coupled the Fast-J radiative transfer model with GEOS-CHEM, while *Feng et al.* [2004] calculated photolysis frequencies with a linear or quasi-linear interpolation from a table of calculated photolysis frequencies for specified clear or cloudy conditions. They reported the global average errors in the cloudy-sky look-up table photolysis frequencies $J[O^1D]$ and $J[NO_2]$ are between -6% and +1% when compared to the exact method. These errors are on the order of the difference between RAN and MRAN (**Figures 8 and 9**) and therefore are relatively large. As our results have shown, the differences of photolysis frequencies above clouds or in the upper portion of clouds between using RAN and MRAN should be smaller than those between using LIN and MRAN, since LIN allows less solar radiation to penetrate down below the cloud. However, the results of *Feng et al.* [2004] seemed to show the former is larger than the latter for $J[O^1D]$ in the tropics (see their Figure 7), reflecting the relatively large errors due to parameterized calculation of photolysis rates in their table look-up scheme. This suggests the importance of coupling the radiative transfer model with CTMs. Second, we included the full O_3-NO_x-CO-VOC chemistry in our simulations while *Feng et al.* [2004] used prescribed concentrations of O_3, NO_x, CO and other long-lived species. Our simulated effect of cloud overlap on OH should therefore be more consistent with the effect of clouds on other trace species.

Cloud overlap assumptions used in the model have a significant influence on the calculated total cloud cover and radiation fields [*Morcrette and Jakob*, 2000; *Bergman and Rasch*, 2002; *Stephens et al.*, 2004]. Observations studies however did not prefer any of the cloud assumptions (see the review of *Feng et al.*, 2004). In fact, existing overlap assumptions have significant limitations that may lead to unrealistic cloud distributions [*Bergman and Rasch*,

2002; *Stephens et al.*, 2004]. For instance, *Stephens et al.* [2004] demonstrated that the random and maximum-random overlap methods create a vertical-resolution-dependent bias in model total cloudiness and radiative fluxes. Since GEOS-CHEM is an offline model, we do not include in our calculation the impact of cloud overlap on radiation fields of the atmosphere, nor do we try to examine which cloud overlap assumption gives better total cloudiness and surface and top-of-the-atmosphere radiation fluxes. We suggest using online CTMs to address the issue. On the other hand, current satellite observations of global cloudiness also suffer from multi-layered cloud systems due to its assumption that only a single cloud layer is present in a given pixel. The potential for using satellites to detect cloud overlap however is encouraging [*Pavolonis and Heidinger*, 2004].

8. Summary and Conclusions

We have used a state-of-the-art global 3-D model of tropospheric chemistry driven by assimilated meteorological data (GEOS-3) coupled with the Fast-J radiative transfer model [*Wild et al.*, 2000] to assess the radiative effect of clouds on photolysis frequencies and key oxidants in the troposphere during 2001. Our aim was to improve our quantitative understanding of this effect on a global scale, including the associated uncertainties due to different cloud overlap assumptions. Three different methods are used to assess the impact of clouds on radiative transfer and they are the uniform cloud distribution method (linear assumption or LIN), an approximate random overlap assumption (RAN), and the maximum-random overlap assumption (MRAN).

To properly take into account the radiative effect of clouds, we have evaluated GEOS-3 column cloud optical depth and cloud fraction with MODIS and ISCCP satellite retrieval

products. We showed that MODIS and ISCCP monthly mean cloud optical depths (linear averages of pixel values) are actually comparable in magnitude. GEOS-3 cloud optical depths show peaks in the tropics associated with deep convective clouds and at midlatitudes associated with extratropical cyclones in NH and marine stratiform clouds in SH. These features reasonably agree with MODIS and ISCCP cloud retrieval products, although GEOS-3 tends to overestimate cloud optical depths in the tropics and SH midlatitudes. GEOS-3 cloud fraction agrees with MODIS and ISCCP products but appears lower at midlatitudes.

While we have been able to reproduce with Fast-J the one-dimensional test cases for the radiative effect of clouds on photolysis rates in the literature, our online simulation results of the global impact of clouds on photolysis frequencies are significantly different than those of previous studies in many aspects. Our calculation shows that globally averaged photolysis frequencies $J[O^1D]$, $J[NO_2]$ and $J[CH_2O]$ in the troposphere are reduced by only ~2-4% due to the impact of clouds with the use of any of the cloud overlap assumptions, reflecting an offsetting effect of above-cloud enhancements due to reflection of solar radiation and below-cloud reductions. This small global average effect and insensitivity to cloud overlap are in distinct contrast with a global modeling study using MOZART-2 [*Tie et al.*, 2003] where a global average enhancement of 13% (~45-62%) was found using MRAN (LIN). Despite the insensitivity of the global average effect to cloud overlap, we do find that LIN significantly overestimates the above-cloud enhancements and the below-cloud reductions when compared to RAN or MRAN, consistent with the findings of *Feng et al.* [2004]. However, our calculated differences in photolysis frequencies between LIN, RAN or MRAN are more consistent with these cloud overlap schemes themselves.

Consistent with the previous studies [*Tie et al.*, 2003; *Feng et al.*, 2004], our calculations indicate that clouds have important effects on tropospheric chemistry through modification of photolysis frequencies. However, our results highlight that the dominant radiative effect of clouds is to influence the vertical redistribution of the intensity of photochemical activity while the global average effect remains modest. This contrasts with the result of *Tie et al.* [2003]. Differing vertical distributions of clouds may explain part, but not majority, of the discrepancies between models.

Specifically, our calculated global mean changes in OH, O_3, NO_x, HO_2, CH_2O, and CO due to clouds are generally less than 6% using any of the cloud overlap assumptions. For OH, the global mean change is insignificant (~1%) but it shows much larger changes above (5-10%) and below (- 5-20%) the tropical deep convective clouds and the midlatitude low level clouds, as well as near the surface (~ -20%). The global mean lifetime of CH_3CCl_3 (CH_4) increases by ~3-5% from a clear-sky value of 6.5 (11) years; the positive impact of clouds reflects the fact that the lifetime of CH_3CCl_3 (CH_4) is more sensitive to OH in the lower troposphere where clouds strongly decrease OH concentrations. For O_3, the global mean effect is about 3-5% increase. O_3 increases occur in most of the troposphere with maximum in the tropical upper troposphere, consistent with *Tie et al.* [2003]. Our calculated O_3 increase in the tropical upper troposphere (~5-8%) is however substantially smaller than that (~20-30%) of Tie et al. [2003]. While O_3 increases above the clouds in our model reflect the increased net O_3 production due to backscattering of solar radiation, O_3 increases below the tropical deep clouds and the SH marine stratus are a result of reduced net O_3 losses in these regimes. The radiative effect of clouds on CO is not significant both globally and regionally in the vertical (~1-2%), reflecting that loss of CO by OH is partly compensated by CO production from hydrocarbons.

Our model results using different cloud overlap assumptions do not indicate which assumption is preferred, although one may argue that MRAN is more realistic. Relative to MRAN, LIN significantly overestimates the impact of clouds on tropospheric chemistry. We find that RAN ($\tau_c' = \tau_c \cdot f^{3/2}$) is a good approximation of MRAN in terms of the radiative impact of clouds on tropospheric chemistry. Since RAN is computationally much cheaper than MRAN, RAN is a good compromise between including the effect of cloud overlap and achieving computational efficiency.

The radiative effect of clouds on tropospheric chemistry in a global CTM critically depends on the cloud optical properties and, in particular, on the vertical distribution of cloud optical depth and cloud fraction, which is still one of the largest uncertainties in current general circulation models and other meteorological products. For instance, there are important differences between the vertical distributions of cloud optical depth in the GEOS-3 and GEOS-4 meteorological archives, leading to significant differences in the simulated OH (oxidation capability) in the troposphere. Assimilating satellite observations of cloud optical properties in global models may help reduce such uncertainties. In particular, with the launchings of CALIPSO and CloudSat, a unique data set of cloud optical and physical properties as well as their vertical distribution will substantially improve our constraints on the radiative effect of clouds on tropospheric chemistry and climate. Eventually it will lead us to an improved understanding of cloud-chemistry-climate interactions in a changing climate.

Acknowledgments. This research was supported by NASA Langley Research Center. We would like to thank William Rossow, Patrick Minnis and Paul Hubanks for useful suggestions, Joyce Penner, Daniel Jacob and three anonymous reviewers for helpful comments, Lawrence Takacs and Man-Li Wu for helping us understand the GEOS-3 archive, and Oliver Wild for discussions about Fast-J. MODIS and ISCCP products are distributed by NASA Goddard Distributed Active Archive Center and Langley Atmospheric Sciences Data Center, respectively. The GEOS-CHEM model is managed by the Atmospheric Chemistry Modeling Group at Harvard University with support from the NASA Atmospheric Chemistry Modeling and Analysis Program (ACMAP).

References

Allen, D. J., R. B. Rood, A. M. Thompson, and R. D. Hudson (1996), Three-dimensional radon 222 calculations using assimilated meteorological data and a convective mixing algorithm, *J. Geophys. Res., 101*, 6871-6881.

Berntsen, T.K., and I.S.A. Isaksen (1997), A global three-dimensional chemical transport model for the troposphere. 1. Model description and CO and ozone results, *J. Geophys. Res., 102*, 21,239-21,280.

Bey I., D. J. Jacob, R. M. Yantosca, J. A. Logan, B. Field, A. M. Fiore, Q. Li, H. Liu, L. J. Mickley, and M. Schultz (2001a), Global modeling of tropospheric chemistry with assimilated meteorology: Model description and evaluation, *J. Geophys. Res., 106*, 23,073-23,096.

Bey I., D. J. Jacob, J. A. Logan, and R. M. Yantosca (2001b), Asian chemical outflow to the Pacific: Origins, pathways and budgets, *J. Geophys. Res., 106*, 23,097-23,114.

Bergman, J.W., and P.J. Rasch (2002), Parameterizing vertically coherent cloud distributions, *J. Atmos. Sci., 59*, 2165-2182.

Brasseur, G.P., D.A., Hauglustaine, S. Walters, P.J. Rasch, J.-F. Muller, C. Granier, and X. Tie (1998), MOZART, a global chemical tracer model for ozone and related chemical tracers. 1. Model description, *J. Geophys. Res., 103*, 28,265-28,289.

Briegleb, B.P. (1992), Delta-eddington approximation for solar radiation in the NCAR Community Climate Model, *J. Geophys. Res., 97*, 7603-7612.

Cess, R.D., and 33 co-authors (1996), Cloud feedback in atmospheric general circulation models: An update, *J. Geophys. Res., 101*, 12,791-12,794.

Chandra, S., J.R. Ziemke, and R.V. Martin (2003), Tropospheric ozone at tropical and middle latitudes derived from TOMS/MLS residual: Comparison with a global model, *J. Geophys. Res., 108*(D9), 4291, doi:10.1029/2002JD002912.

Collins, W.D. (2001), Parameterization of generalized cloud overlap for radiative calculations in general circulation models, *J. Atmos. Sci., 58*, 3224-3242.

Crawford, J.H., D. Davis, G. Chen, R. Shetter, M. Muller, J. Barrick, and J. Olson (1999), An assessment of cloud effects on photolysis rates: Comparison of experimental and theoretical values, *J. Geophys. Res., 104*, 5725-5734.

Douglass, A.R., M.J. Prather, T.M. Hall, S.E. Strahan, P.J. Rasch, L.C. Sparling, L. Coy, and J.M. Rodriguez (1999), Choosing meteorological input for the global modeling initiative assessment of high-speed aircraft, *J. Geophys. Res., 104*, 27,545-27,564.

Duncan, B.N., R.V. Martin, A.C. Staudt, R. Yevich, J.A. Logan (2003), Interannual and seasonal variability of biomass burning emissions constrained by satellite observations, *J. Geophys. Res., 108*(D2), 4040, doi:10.1029/2002JD002378.

Feng, Y., J.E. Penner, S. Sillman, and X. Liu (2004), Effects of cloud overlap in photochemical models, *J. Geophys. Res., 109*, D04310, doi:10.1029/2003JD004040.

Fiore, A.M., D.J. Jacob, I. Bey, R.M. Yantosca, B.D. Field, A.C. Fusco, and J.G. Wilkinson (2002a), Background ozone over the United States in summer: Origin, trend, and contribution to pollution episodes, *J. Geophys. Res., 107*(D15), doi:10.1029/2001JD000982.

Fiore, A.M., D.J. Jacob, B.D. Field, D.G. Streets, S.D., Fernandes, and C. Jang (2002b), Linking ozone pollution and climate change: The case for controlling methane, *Geophys. Res. Lett., 29*(19), doi:10.1029/2002GL015601.

Fiore, A.M., D.J. Jacob, R. Mathur, R.V. Martin (2003a), Application of empirical orthogonal functions to evaluate ozone simulations with regional and global models, *J. Geophys. Res., 108*, 4431, doi:10.1029/2002JD003151.

Fiore, A.M., D.J. Jacob, H. Liu, R.M. Yantosca, T.D. Fairlie, and Q. Li (2003b), Variability in surface ozone background over the United States: Implications for air quality policy, *J. Geophys. Res., 108*(D24), 4787, doi:10.1029/2003JD003855.

Geleyn, J.F., and A. Hollingsworth (1979), An economical analytical method for the computation of the interaction between scattering and line absorption of radiation, *Contrib. Atmos. Phys., 52*, 1-16.

Hartmann, D.L., C.S. Bretherton, T.P. Charlock, M.D. Chou, A. Del Genio, R.E. Dickinson, R. Fu, R.A. Houze, M.D. King, K.M. Lau, C.B. Leovy, S. Sorooshian, J. Washburne, B. Wielicki, and R.C. Willson (1999), Chapter 2. Radiation, clouds, water vapor, precipitation, and atmospheric circulation, in *EOS Science Plan: The State of Science in the EOS Program*, edited by Michael D. King, pp.397, National Aeronautics and Space Administration, NP-1998-12-069-GSFC, January.

Herman, J.R., and E.A. Celarier (1997), Earth surface reflectivity climatology at 340-380 nm from TOMS data, *J. Geophys. Res., 102*, 28,003-28,011.

Hogan, R.J., and A.J. Illingworth (2000), Deriving cloud overlap statistics from radar observations, *Q. J. R. Meteorol. Soc., 126*, 1-7.

Horowitz, L.W., et al. (2003), A global simulation of tropospheric ozone and related tracers: Description and evaluation of MOZART, version 2, *J. Geophys. Res., 108*(D24), 4784, doi:10.1029/2002JD002853.

Houghton, J.T., Y. Ding, D.J. Griggs, M. Noguer, P.J. van der Linden, and D. Xiaosu, Eds. (2001), *Climate Change 2001: The Scientific Basis*, Cambridge University Press, 944pp.

Jacob, D.J. (2000), Heterogeneous chemistry and tropospheric ozone, *Atmos. Environ., 34*, 2131-2159.

Jacob, D.J., E.W. Gottlieb, and M.J. Prather (1989), Chemistry of a polluted cloudy boundary layer, *J. Geophys. Res., 94*, 12,975-13,002.

Jakob, C., and S.A. Klein (1999), The role of vertically varying cloud fraction in the parameterization of microphysical processes in the ECMWF model, *Q. J. R. Meteorol. Soc., 125*(555), 941-965.

Junkermann, W. (1994), Measurements of the $J(^1D)$ actinic flux within and above stratiform clouds and above snow surfaces, *Geophys. Res. Lett., 21*, 793-796.

Landgraf, J., and P.J. Crutzen (1998), An Efficient method for online calculations of photolysis and heating rates, *J. Atmos. Sci., 55*, 863-878.

Lefer, B.L., R.E. Shetter, S.R. Hall, J.H. Crawford, and J.R. Olson (2003), Impact of clouds and aerosols on photolysis frequencies and photochemistry during TRACE-P: 1. Analysis using radiative transfer and photochemical box models, *J. Geophys. Res., 108*, doi:10.1029/2002JD003171.

Liang, X.-Z., and W.-C. Wang (1997), Cloud overlap effects on general circulation model climate simulations, *J. Geophys. Res., 102*, 11,039-11,047.

Li, Q., D. J. Jacob, J. A. Logan, I. Bey, R. M. Yantosca, H. Liu, R. V. Martin, A. M. Fiore, B. D. Field, B. N. Duncan, and V. Thouret (2001), A tropospheric ozone maximum over the Middle East, *Geophys. Res. Lett., 28*, 3235-3238.

Li, Q., D.J. Jacob, T.D. Fairlie, H. Liu, R.M. Yantosca, and R.V. Martin (2002a), Stratospheric versus pollution influences on ozone at Bermuda: Reconciling past analyses, *J. Geophys. Res., 107*(D22), doi:10.1029/2002JD002138.

Li, Q., D.J. Jacob, I. Bey, P.I. Palmer, B.N. Duncan, B.D. Field, R.V. Martin, A.M. Fiore, R.M. Yantosca, D.D. Parrish, P.G. Simmonds, and S.J. Oltmans (2002b), Transatlantic transport of pollution and its effects on surface ozone in Europe and North America, *J. Geophys. Res., 107*(D13), doi:10.1029/2001JD001422.

Liang, X.-Z., and W.-C. Wang, Cloud overlap effects on general circulation model climate simulations, *J. Geophys. Res., 102*(D10), 11,039-11,047, 1997.

Lin, S.-J., and R.B. Rood (1996), Multidimensional flux-form semi-Lagrangian transport schemes, *Mon. Weather Rev., 124*, 2046-2070.

Liu, H., D. J. Jacob, I. Bey, and R. M. Yantosca (2001), Constraints from ^{210}Pb and ^{7}Be on wet deposition and transport in a global three-dimensional chemical tracer model driven by assimilated meteorological fields, *J. Geophys. Res., 106*, 12,109-12,128.

Liu, H., D.J. Jacob, L.Y. Chan, S.J. Oltmans, I. Bey, R.M. Yantosca, J.M. Harris, B.N. Duncan, and R.V. Martin (2002), Sources of tropospheric ozone along the Asian Pacific Rim: An analysis of ozonesonde observations, *J. Geophys. Res., 107*(D21), doi:10.1029/2001JD002005.

Liu, H., D.J. Jacob, J.E. Dibb, A.M. Fiore, and R.M. Yantosca (2004), Constraints on the sources of tropospheric ozone from ^{210}Pb-^{7}Be-ozone correlations, *J. Geophys. Res., 109*, D07306, doi:10.1029/2003JD003988.

Mao, H., W.-C. Wang, X.-Z., Liang, and R.W. Talbot (2003), Global and seasonal variations of O_3 and NO_2 photodissociation rate coefficients, *J. Geophys. Res., 108*(D7), 4216, doi:10.1029/2002JD002760.

Martin, R.V., D.J. Jacob, J.A. Logan, I. Bey, R.M. Yantosca, A.C. Staudt, Q.B. Li, A.M. Fiore, B.N. Duncan, H. Liu, P. Ginoux, and V. Thouret (2002), Interpretation of TOMS observations of tropical tropospheric ozone with a global model and in situ observations, *J. Geophys. Res., 107*(D18), 4351, 10.1029/2001JD001480.

McLinden, C.A., S.C. Olsen, B. Hannegan, O. Wild, M.J. Prather, and J. Sundet (2000), Stratospheric ozone in 3-D models: A simple chemistry and the cross-tropopause flux, *J. Geophys. Res., 105*, 14,653-14,665.

Morcrette, J.-J., and C. Jakob (2000), The response of the ECMWF model to changes in the cloud overlap assumption, *Mon. Weather Rev., 128*, 1707-1732.

Olson, J., et al. (1997), Results from the Intergovernmental Panel on Climatic Change Photochemical Model Intercomparison (PhotoComp), *J. Geophys. Res., 102*, 5979-5991.

Park R. J., D. J. Jacob, B. D. Field, R. M. Yantosca, and M. Chin (2004), Natural and transboundary pollution influences on sulfate-nitrate-ammonium aerosols in the United States: Implications for policy, *J. Geophys. Res., 109*, D15204, doi:10.1029/2003JD004473.

Pavolonis, M.J., and A.K. Heidinger (2004), Daytime cloud overlap detection from AVHRR and VIIRS, *J. Appl. Meteor., 43*, 762-778.

Penner, J.E., C.S. Atherton, J. Dignon, S.J. Ghan, J.J. Walton, and S. Hameed (1991), Tropospheric nitrogen - A three-dimensional study of sources, distributions, and deposition, *J. Geophys. Res., 96*, 959-990.

Pickering, K.E., et al. (1998), Vertical distributions of lightning NO_x for use in regional and global chemical transport models, *J. Geophys. Res., 103*(D23), 31,203-31,216, doi:10.1029/98JD02651.

Pinker, R., H. Wang, M. King, and S. Platnick (2003), First use of MODIS data to cross-calibrate with GEWEX/SRB data sets, *Global Energy and Water Cycle Experiment (GEWEX) News*, *13*(4), 4-5.

Platnick, S., M.D. King, S.A. Ackerman, W.P. Menzel, B.A. Baum, J.C. Riedi, and R.A. Frey (2003), The MODIS cloud products: Algorithms and examples from Terra, *IEEE Transactions on Geoscience and Remote Sensing, 41*(2), 459-473.

Prather, M., and D. Jacob (1997), A persistent imbalance in HO_x and NO_x photochemistry of the upper troposphere driven by deep tropical convection, *Geophys. Res. Lett., 24*, 3189-3192.

Prinn, R.G., et al. (2001), Evidence for substantial variations of atmospheric hydroxyl radicals in the past two decades, *Science, 292*, 1882-1888.

Rossow, W.B., A.W. Walker, D.E. Beuschel, M.D. Roiter (1996), *International Satellite Cloud Climatology Project (ISCCP) Documentation of New Cloud Datasets*, International Council of Scientific Unions and World Meteorological Organization, January.

Rossow, W.B., and R.A. Schiffer (1999), Advances in understanding clouds from ISCCP. *Bull. Am. Meteorol. Soc.*, *80*, 2261-2287.

Shindell, D. T., J. L. Grenfell, D. Rind, and V. Grewel (2001), Chemistry-climate interactions in the Goddard Institute for Space Studies general circulation model, 1, Tropospheric chemistry description and evaluation, *J. Geophys. Res., 106*, 8047-8075.

Slingo, A., and H. Schrecker (1982), On the short-wave radiative properties of stratiform water clouds, *Q. J. R. Meteorol. Soc., 108*, 407-426.

Spivakovsky, C.M., R. Yevich, J.A. Logan, S.C. Wofsy, and M.B. McElroy (1990), Tropospheric OH in a three-dimensional chemical tracer model: An assessment based on observations of CH_3CCl_3, *J. Geophys. Res., 95*, 18,441-18,471.

Spivakovsky, C. M., et al. (2000), Three-dimensional climatological distribution of tropospheric OH: Update and evaluation, *J. Geophys. Res., 105*, 8931-8980.

Stephens, G.L., N.B. Wood, and P.M. Gabriel (2004), An assessment of the parameterization of subgrid-scale cloud effects on radiative transfer. Part I: vertical overlap, *J. Atmos. Sci., 61*, 715-732.

Stubenrauch, C.J., A.D. Del Genio, and W.B. Rossow (1997), Implementation of subgrid cloud vertical structure inside a GCM and its effect on the radiation budget, *J. Clim., 10*, 273-287.

Tang, Y., et al. (2003), Impacts of aerosols and clouds on photolysis frequencies and photochemistry during TRACE-P: 2. Three-dimensional study using a regional chemical transport model, *J. Geophys. Res.*, *108*, 8822, doi:10.1029/2002JD003100.

Thompson, A. M. (1984), The effect of clouds on photolysis rates and ozone formation in the unpolluted troposphere, *J. Geophy. Res., 89*, 1341-1349.

Thompson, A. M., M. A. Huntley, and R. W. Stewart (1990), Perturbations of tropospheric oxidants, 1985-2035: Calculations of ozone and OH in chemically coherent regions, *J. Geophys. Res., 95*, 9829-9844.

Tie, X., S. Madronich, S. Walters, R. Zhang, P. Rasch, and W. Collins (2003), Effect of clouds on photolysis and oxidants in the troposphere, *J. Geophys. Res., 108*(D20), 4642, doi:10.1029/2003JD003659.

Tie, X., S. Madronich, S. Walters, R. Zhang, P. Rasch, and W. Collins (2006), Correction to "Effect of clouds on photolysis and oxidants in the troposphere", submitted to *J. Geophys. Res.*

Wild, O., X. Zhu, and M.J. Prather (2000), Fast-J: Accurate simulation of in- and below-cloud photolysis in tropospheric chemical models, *J. Atmos. Chem., 37*, 245-282.

Yang, H., and H. Levy (2004), Sensitivity of photodissociation rate coefficients and O_3 photochemical tendencies to aerosols and clouds, *J. Geophys. Res., 109*(D24), D24301, doi: 10.1029/2004JD005032.

Table 1. Percentage changes in J[O^1D] and J[NO_2] due to clouds calculated with the off-line Fast-J model and maximum-random overlap (MRAN) scheme[a], as a function of cloud vertical distribution, cloud liquid water content (LWC), and solar zenith angle (SZA).

SZA	cloud vertical distribution	LWC (g/m^3)		
		0.05	0.10	0.15
0°	low cloud[b]	12.5[c] (21.0[d])	18.7 (31.1)	22.2 (36.6)
	high cloud[b]	3.8 (7.7)	1.5 (5.9)	-0.7 (4.0)
	multi-layer cloud[b]	15.6 (28.9)	18.1 (36.1)	18.4 (39.0)
30°	low cloud	11.3 (18.6)	16.3 (26.5)	19.2 (30.9)
	high cloud	0.0 (2.9)	-2.9 (0.3)	-4.9 (-1.5)
	multi-layer cloud	10.5 (21.2)	11.7 (25.7)	11.7 (27.7)
60°	low cloud	7.8 (13.1)	10.7 (16.7)	12.5 (18.7)
	high cloud	-8.9 (-8.9)	-11.8 (-11.4)	-13.4 (-12.8)
	multi-layer cloud	-1.7 (2.4)	-2.0 (3.1)	-2.2 (3.7)
75°	low cloud	5.6 (6.7)	8.0 (8.7)	9.4 (9.8)
	high cloud	-12.9 (-15.1)	-15.1 (-16.6)	-16.4 (-17.4)
	multi-layer cloud	-7.4 (-9.1)	-7.4 (-8.8)	-7.4 (-8.5)

[a]Atmospheric conditions are based on those of tropical regions (13°N). Surface albedo is 0.1. Total ozone column is 258.6DU. Cloud fraction is 50%. See text for details.

[b]Three different vertical distributions of clouds (after *Tie et al.* [2003]). Low cloud case: a single cloud layer between 0-3km; High cloud case: a single cloud layer between 9-11km; Multi-layer cloud case: two cloud layers between 0-3km and 9-11km.

[c]Percentage changes of 0-16km averages for J[O^1D].

[d]Percentage changes of 0-16km averages for J[NO_2].

Table 2. Simulated percentage changes in the global mean concentrations of tropospheric chemical species, photolysis frequencies and global mean lifetimes of methylchloroform (MCF) and CH_4 due to the radiative effect of clouds with different cloud overlap assumptions (LIN, RAN, and MRAN) in June and December 2001, following Table 4 of *Tie et al.* [2003]. The radiative effect of clouds is represented by subtraction of the clear-sky simulation from the cloudy-sky simulation.

Quantity	GEOS-CHEM[a] (this work)			MOZART-2[b] [*Tie et al.*, 2003]	
June					
	LIN	RAN	MRAN	LIN	MRAN
OH	0.99	0.13	-0.52	88.09	20.31
O_3[c]	4.8	3.15	3.65	12.07	8.55
NO_x[d]	5.58	3.46	3.26	-4.17	-3.13
HO_2	-2.27	-1.60	-1.47	16.52	5.89
CH_2O	5.55	3.85	4.77	-14.56	-5.78
CO	0.81	1.33	2.26	-31.40	-9.01
$J[O^1D]$	3.23	1.72	0.87	44.98	13.38
$J[NO_2]$	5.80	3.04	3.01	62.24	13.84
$J[CH_2O]$	5.10	2.65	2.67	54.56	13.75
December					
	LIN	RAN	MRAN	LIN	MRAN
OH	11.53	7.21	6.93	80.18	20.57
O_3[c]	3.48	2.05	2.79	12.14	8.53
NO_x[d]	6.72	4.56	3.77	-12.10	-5.60
HO_2	1.89	1.27	1.42	12.11	5.09
CH_2O	3.15	1.81	2.32	-11.90	-4.59
CO	-0.81	-0.15	0.34	-32.43	-10.19
$J[O^1D]$	12.49	7.99	7.84	42.76	12.04
$J[NO_2]$	16.24	10.55	10.52	58.99	13.19
$J[CH_2O]$	14.84	9.46	9.88	51.48	12.40
MCF lifetime[e]	4.97	3.35	4.23	N/A	N/A
CH_4 lifetime[e]	5.38	3.61	4.49	-45[f]	-18[f]

[a]We calculate global mean concentrations by dividing the global total moles of a species by those of air. Global mean photolysis frequencies are volume-weighted values.

[b]Percentage changes reported in *Tie et al.* [2003] were based on the volume mixing ratios

averaged over each grid-box below 200mb (X. Tie, personal communication, 2004). See text for details.

[c]Actually the extended odd oxygen family defined as $O_x = O_3 + NO_2 + 2\times NO_3 +$ peroxyacylnitrates + $HNO_4 + 3\times N_2O_5 + HNO_3$.

[d]$NO_x \equiv NO + NO_2$.

[e]Percentage changes in global annual mean lifetimes of MCF and CH_4. The lifetimes are derived as the ratio of the total burden of atmospheric MCF or CH4 to the tropospheric loss rate against oxidation by OH. Under clear-sky conditions, MCF (CH_4) lifetimes are 6.5 (11) years in GEOS -CHEM, and CH_4 lifetime is about 11.4 years in MOZART-2 [*Tie et al.*, 2003].

[f]Percentage changes averaged over June and December.

FIGURE CAPTIONS

Figure 1. Schematic illustration of implementation of the maximum-random cloud overlap scheme (MRAN) as used by *Tie et al.* [2003] for actinic flux calculations (after *Feng et al.* [2004]). Layers 3, 4, 5 and 9 are cloudy in a ten-layer column. The in-cloud optical depth and cloud fraction at vertical layer i are indicated by τ_i and f_i (i=1, 2, …, 10). This vertical profile of cloudiness is transformed into four configurations. Within the cloud block containing adjacent cloudy layers (i=3, 4, and 5), the cloud fractions are set to the maximum cloud fraction of those layers (f_5), and their cloud optical depths (or water contents) are accordingly adjusted. Actinic fluxes for the original column are the averages of those for all four configurations, weighted by the respective column area fractions.

Figure 2. The global distribution of GEOS-3 monthly mean (grid-scale) cloud optical depths (bottom panel) is compared to ISCCP (D2, 280km equal-area grid, middle panel) and MODIS (MOD08_M3, level-3 monthly global product at 1^ox1^o resolution, top panel) retrievals for March 2001. See text for details.

Figure 3. Same as Figure 2, but shown as zonal mean plots for March, June, October, and December of 2001. MODIS, ISCCP, and GEOS-3 cloud optical depths are thick, thin, and dashed lines, respectively. ISCCP values for October and December are from the year 2000. See text for details.

Figure 4. Same as Figure 3, but for monthly mean cloud fraction. MODIS, ISCCP, and GEOS-3 cloud fractions are thick, thin, and dashed lines, respectively. ISCCP values for October and December are from the year 2000.

Figure 5. Vertical profiles of J[O^1D] at zero solar zenith angles under clear-sky and cloudy conditions calculated by off-line Fast-J for the test cases of *Feng et al.* [2004]. Cloud overlap assumptions are MRAN (maximum-random), RAN (approximate random), and LIN (linear assumption). Clouds are placed between 2-3km and 3-4km (indicated with gray lines): (a). cloud fractions are 0.1 (2-3km) and 0.2 (3-4km) and column mean optical depth is 54; (b). cloud fractions are 0.8 (2-3km) and 0.9 (3-4km) and column mean optical depth is 51; (c). cloud fractions are 0.2 (2-3km) and 0.3 (3-4km) and column mean optical depth is 6.

Figure 6. Same as Figure 5, but at a solar zenith angle of 60º.

Figure 7. Vertical profiles of J[O^1D] at solar zenith angles of (a) 0º, (b) 30º, (c) 60º, and (d) 75º under clear-sky (solid lines) and cloudy (dashed lines, with maximum-random cloud overlap assumption) conditions calculated by off-line Fast-J for the test cases of *Tie et al.* [2003]. Clouds (indicated with gray lines) are placed between 0-3km (single low cloud layer), 9-11km (single high cloud layer), and 0-3km and 9-11km (multi-layer clouds, respectively. Cloud liquid water content is 0.1 g/m3, cloud fraction is 50%, and the effective radius of cloud liquid water droplet is 20μm, following *Tie et al.* [2003, 2006]. See text for details.

Figure 8. Simulated percentage changes in monthly zonal mean J[O^1D] for June 2001 (a) due to the radiative effect of clouds with the linear assumption (LIN), b) due to the radiative effect of clouds with the approximate random overlap (RAN), c) between LIN and the maximum-random overlap (MRAN), and d) between RAN and MRAN. The image in (a) shows the zonal mean GEOS-3 cloud optical depth per kilometer.

Figure 9. Same as Figure 8, but for J[NO_2].

Figure 10. Same as Figures 8abc, but for OH.

Figure 11. Simulated percentage changes in monthly zonal mean (a) O_3 and (b) CO concentrations due to the radiative effect of clouds with the maximum-random cloud overlap assumption for June 2001.

Figure 12. Simulated percentage changes in monthly zonal mean OH concentrations due to the radiative effect of tropical mid- and high- clouds (30^oS-30^oN) for June 2001, as reflected by subtraction of the simulation without tropical mid- and high- clouds from the simulation with global clouds. The linear assumption (LIN) is used.

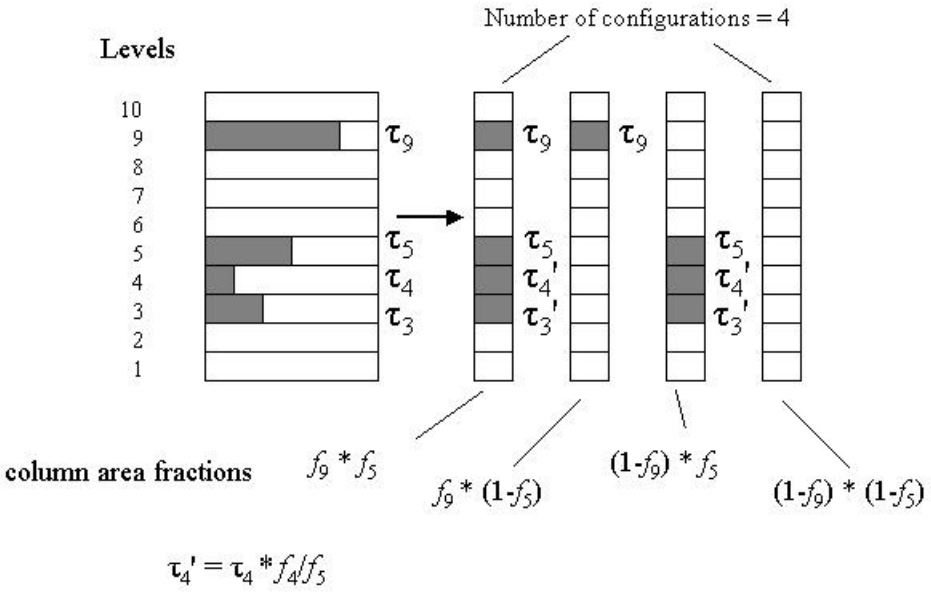

Figure 1. Schematic illustration of implementation of the maximum-random cloud overlap scheme (MRAN) as used by *Tie et al.* [2003] for actinic flux calculations (after *Feng et al.* [2004]). Layers 3, 4, 5 and 9 are cloudy in a ten-layer column. The in-cloud optical depth and cloud fraction at vertical layer i are indicated by τ_i and f_i (i=1, 2, …, 10). This vertical profile of cloudiness is transformed into four configurations. Within the cloud block containing adjacent cloudy layers (i=3, 4, and 5), the cloud fractions are set to the maximum cloud fraction of those layers (f_5), and their cloud optical depths (or water contents) are accordingly adjusted. Actinic fluxes for the original column are the averages of those for all four configurations, weighted by the respective column area fractions.

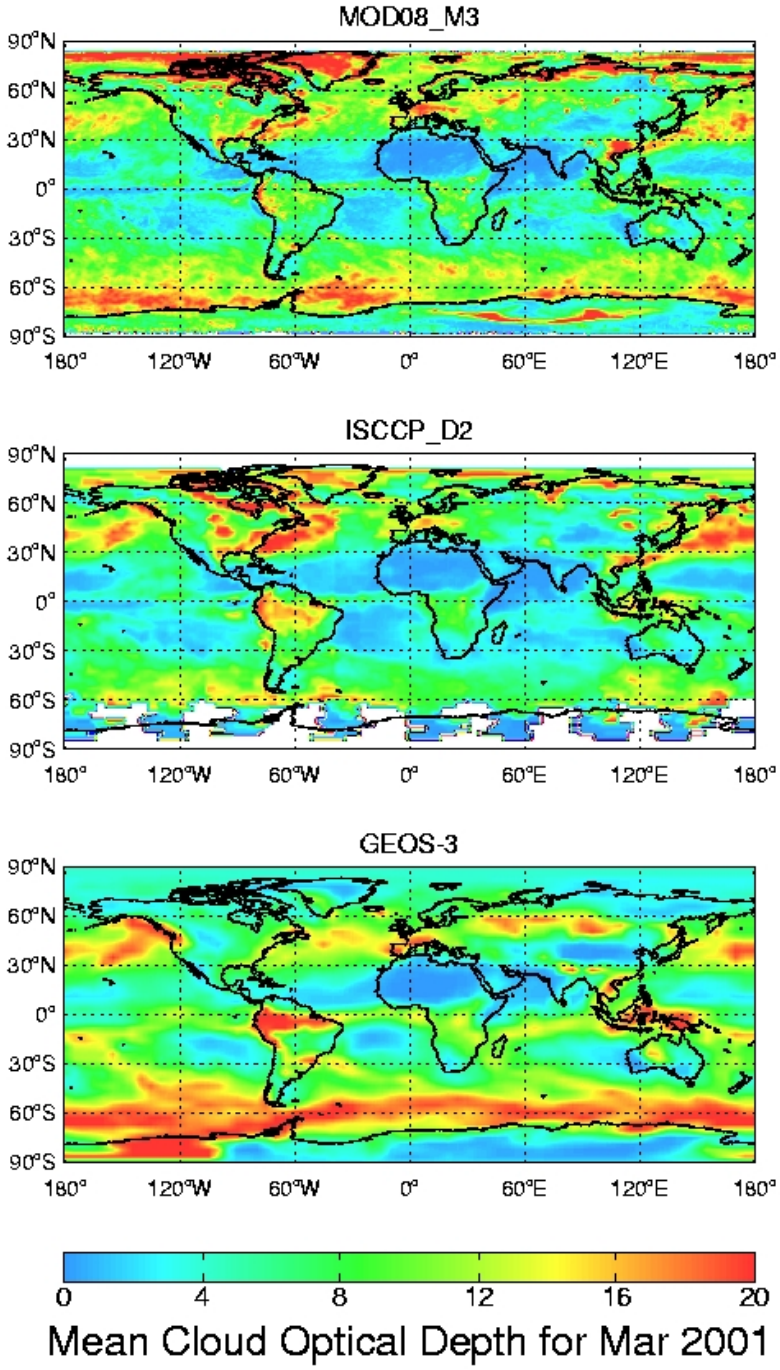

Figure 2. The global distribution of GEOS-3 monthly mean (grid-scale) cloud optical depths (bottom panel) is compared to ISCCP (D2, 280km equal-area grid, middle panel) and MODIS (MOD08_M3, level-3 monthly global product at 1^{o}x1^{o} resolution, top panel) retrievals for March 2001. See text for details.

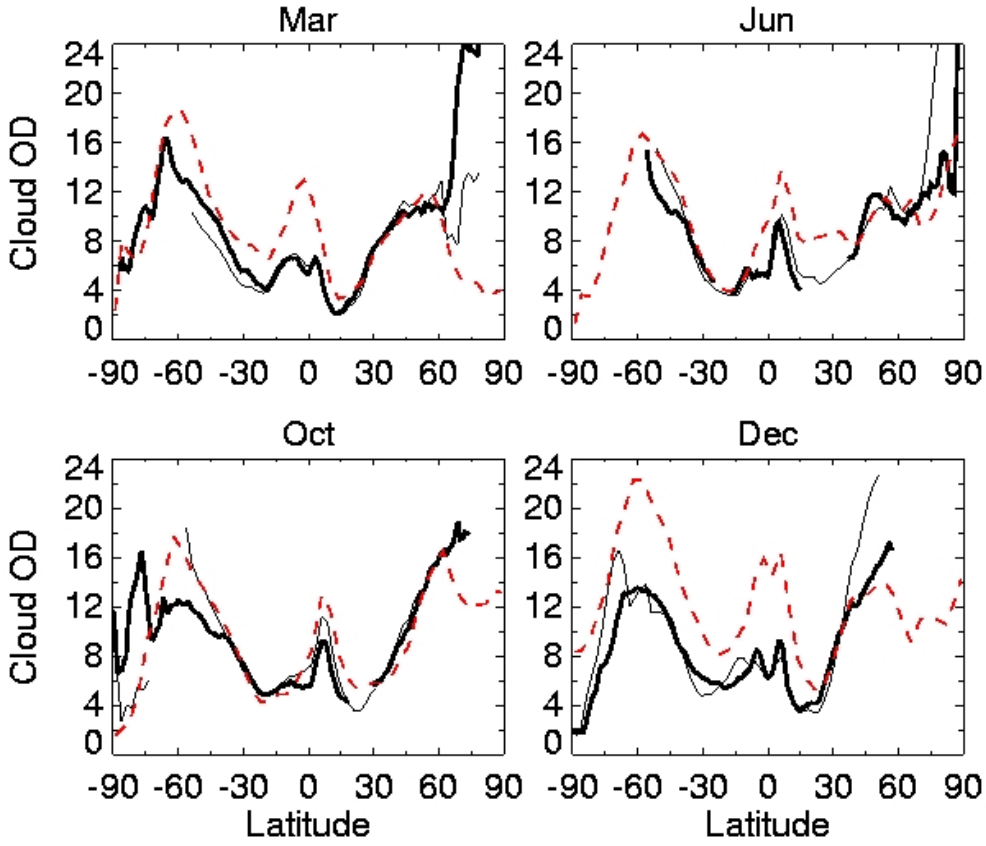

Figure 3. Same as Figure 2, but shown as zonal mean plots for March, June, October, and December of 2001. MODIS, ISCCP, and GEOS-3 cloud optical depths are thick, thin, and dashed lines, respectively. ISCCP values for October and December are from the year 2000. See text for details.

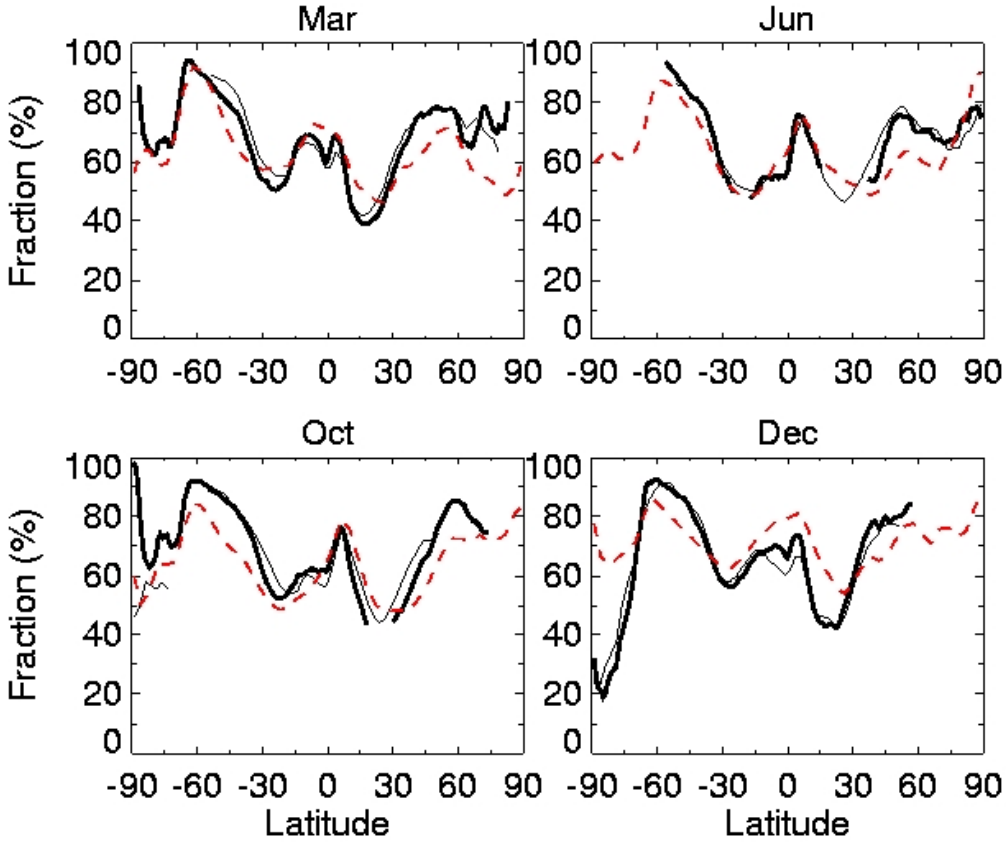

Figure 4. Same as Figure 3, but for monthly mean cloud fraction. MODIS, ISCCP, and GEOS-3 cloud fractions are thick, thin, and dashed lines, respectively. ISCCP values for October and December are from the year 2000.

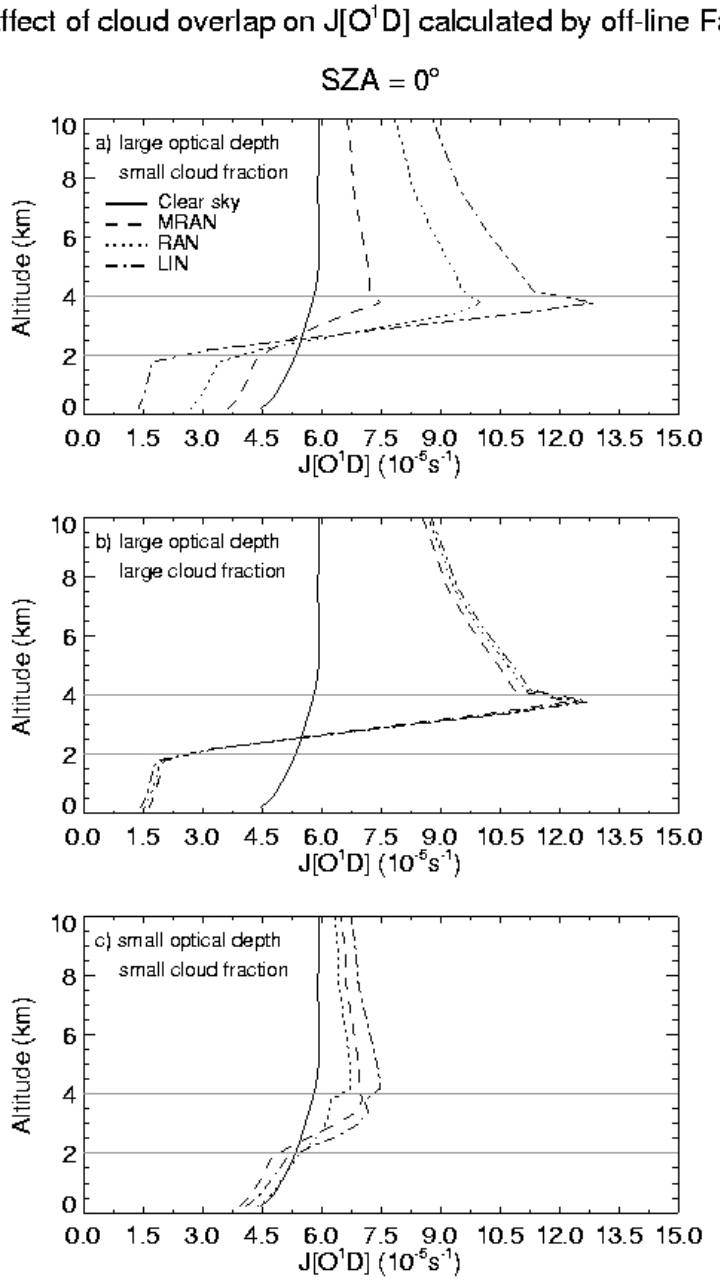

Figure 5. Vertical profiles of J[O^{1}D] at zero solar zenith angles under clear-sky and cloudy conditions calculated by off-line Fast-J for the test cases of *Feng et al.* [2004]. Cloud overlap assumptions are MRAN (maximum-random), RAN (approximate random), and LIN (linear assumption). Clouds are placed between 2-3km and 3-4km (indicated with gray lines): (a). cloud fractions are 0.1 (2-3km) and 0.2 (3-4km) and column mean optical depth is 54; (b). cloud fractions are 0.8 (2-3km) and 0.9 (3-4km) and column mean optical depth is 51; (c). cloud fractions are 0.2 (2-3km) and 0.3 (3-4km) and column mean optical depth is 6.

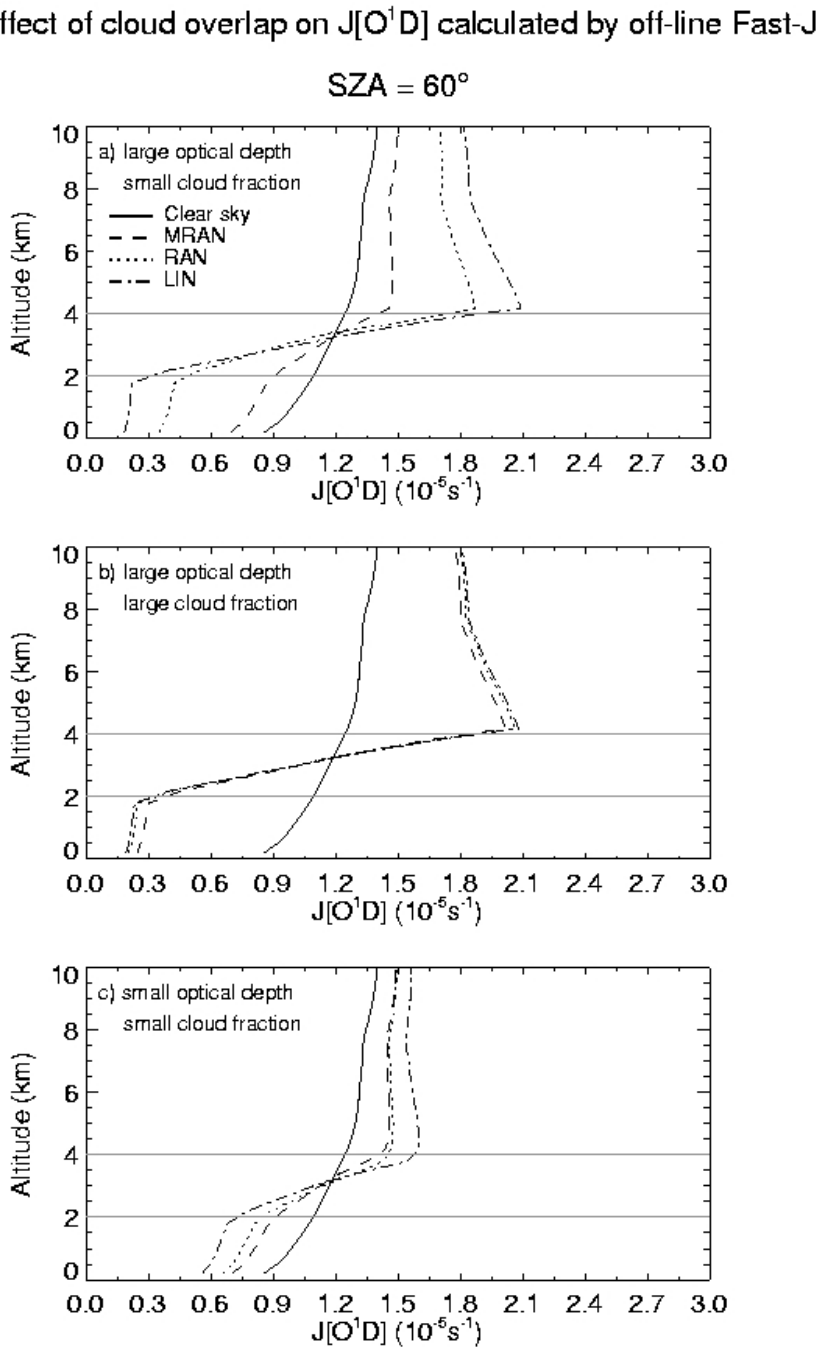

Figure 6. Same as Figure 5, but at a solar zenith angle of 60º.

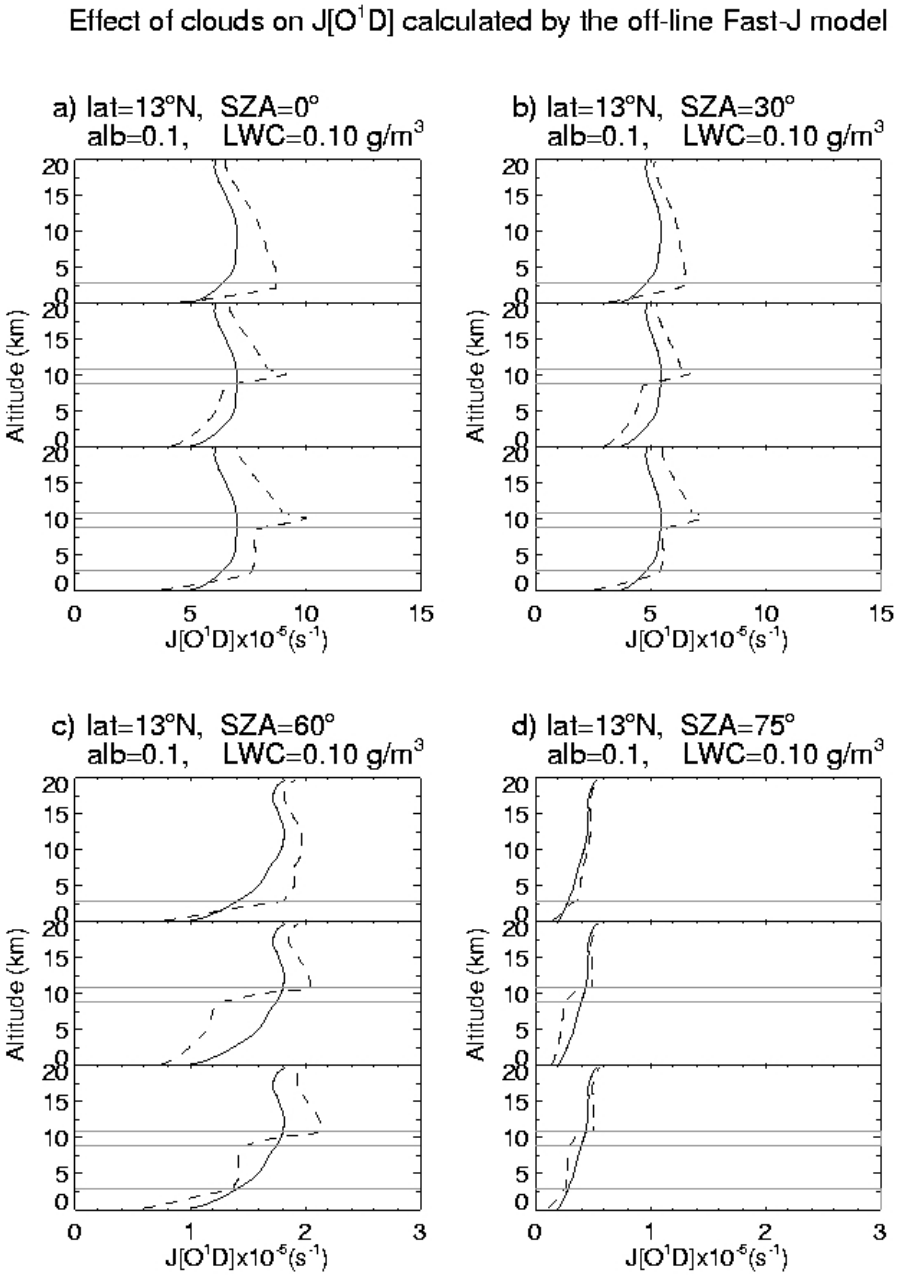

Figure 7. Vertical profiles of J[O^{1}D] at solar zenith angles of (a) 0º, (b) 30º, (c) 60º, and (d) 75º under clear-sky (solid lines) and cloudy (dashed lines, with maximum-random cloud overlap assumption) conditions calculated by off-line Fast-J for the test cases of *Tie et al.* [2003]. Clouds (indicated with gray lines) are placed between 0-3km (single low cloud layer), 9-11km (single high cloud layer), and 0-3km and 9-11km (multi-layer clouds, respectively. Cloud liquid water content is 0.1 g/m3, cloud fraction is 50%, and the effective radius of cloud liquid water droplet is 20μm, following *Tie et al.* [2003, 2006]. See text for details.

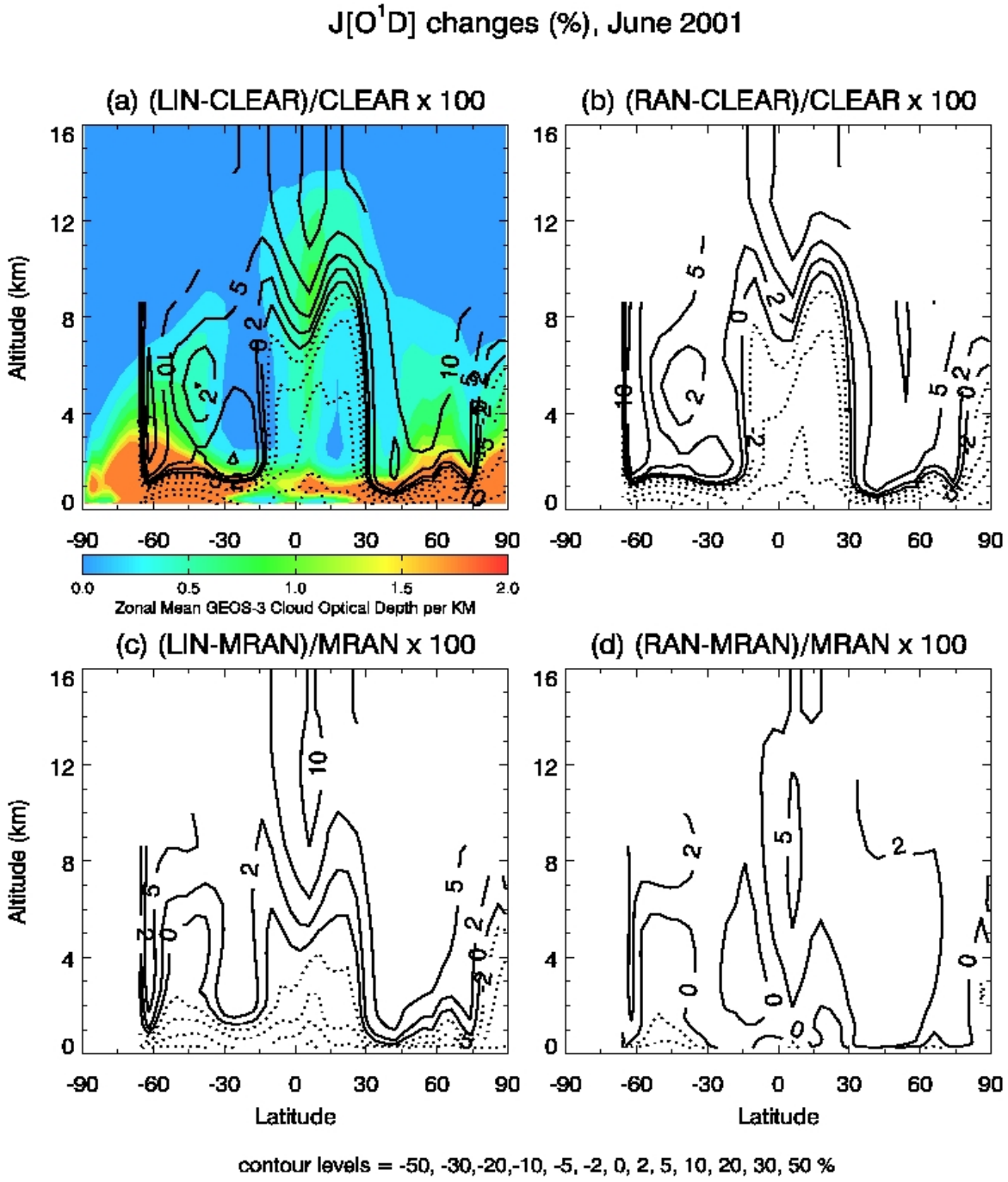

Figure 8. Simulated percentage changes in monthly zonal mean J[O^1D] for June 2001 (a) due to the radiative effect of clouds with the linear assumption (LIN), b) due to the radiative effect of clouds with the approximate random overlap (RAN), c) between LIN and the maximum-random overlap (MRAN), and d) between RAN and MRAN. The image in (a) shows the zonal mean GEOS-3 cloud optical depth per kilometer.

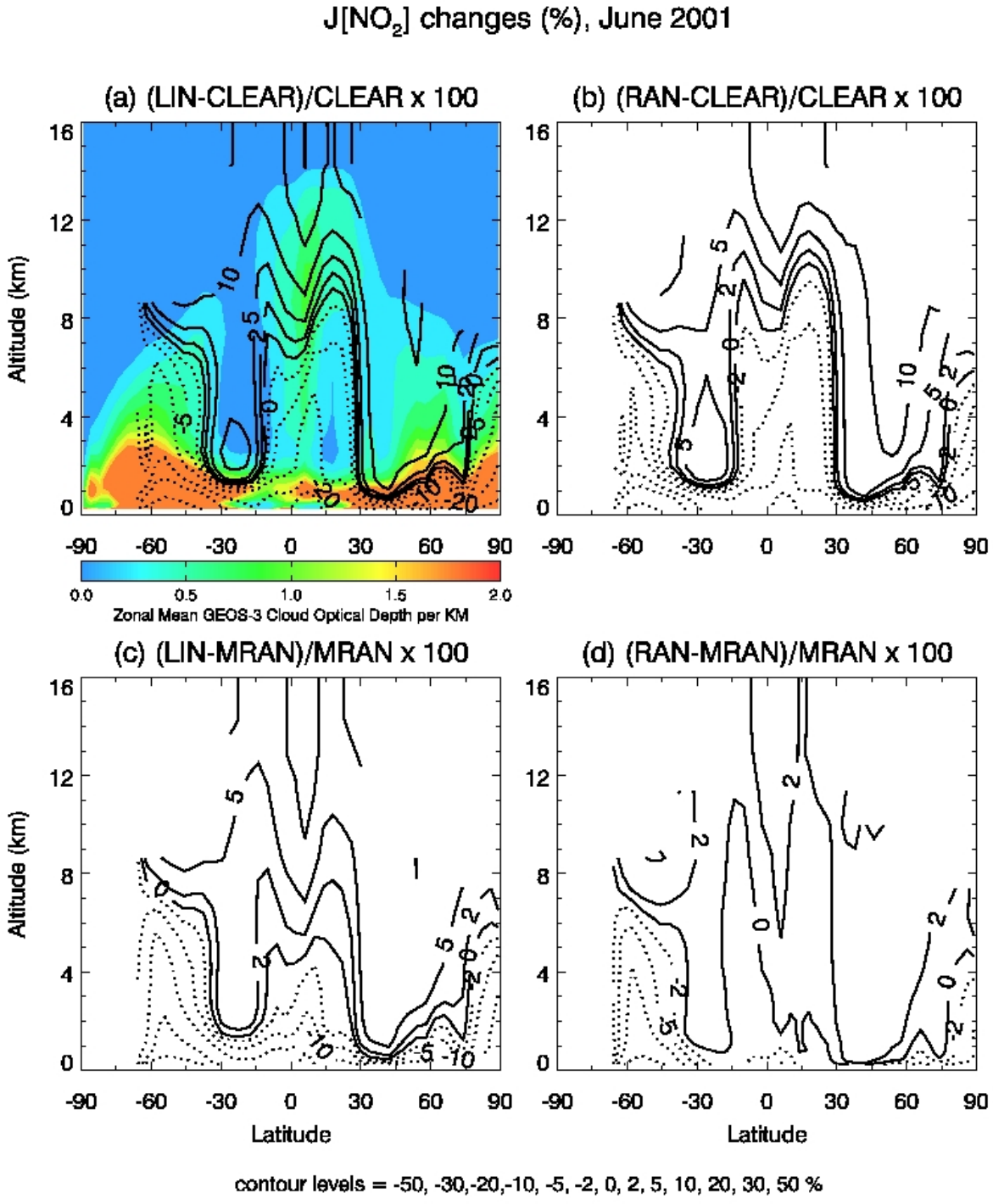

Figure 9. Same as Figure 8, but for J[NO_2].

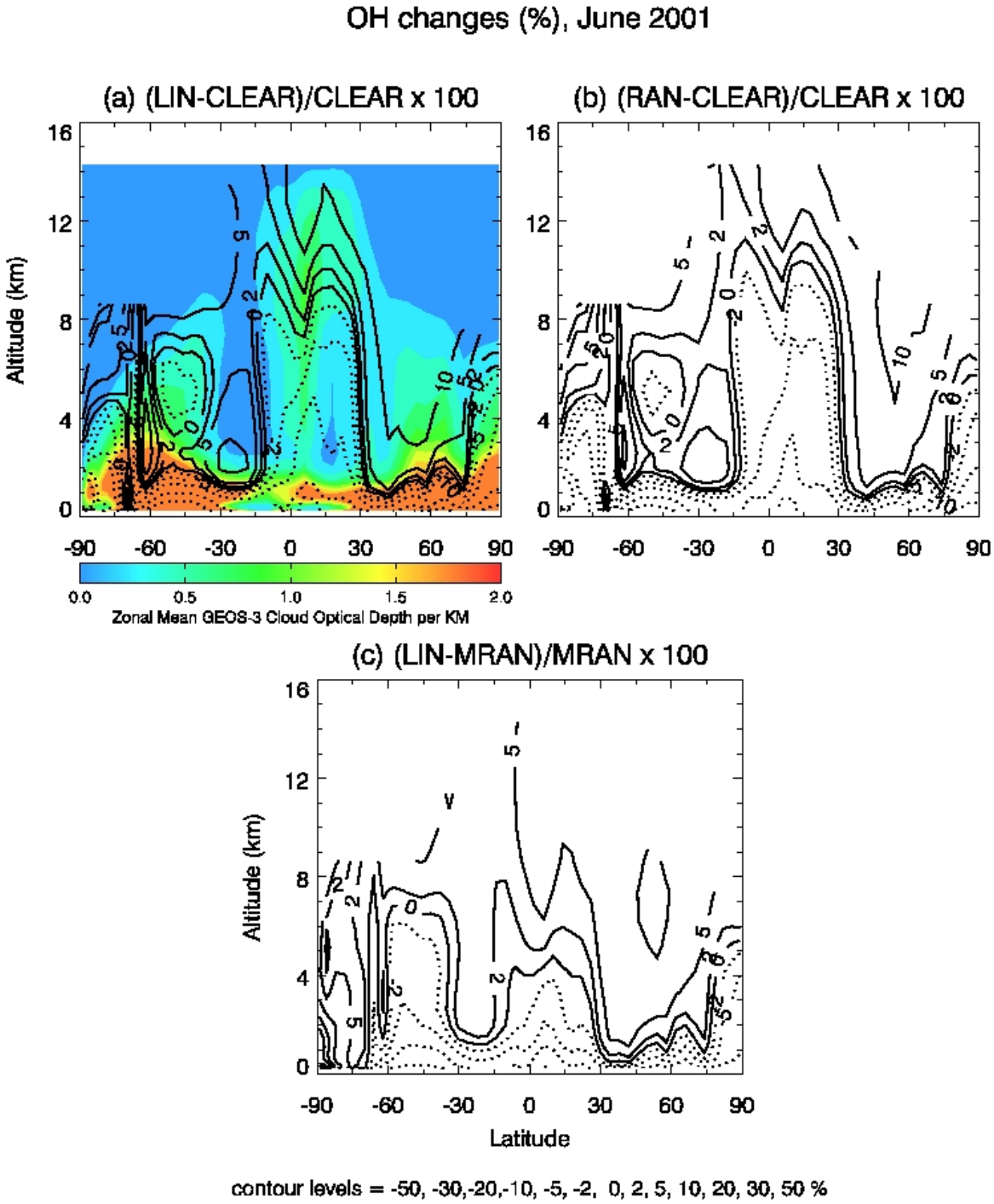

Figure 10. Same as Figures 8abc, but for OH.

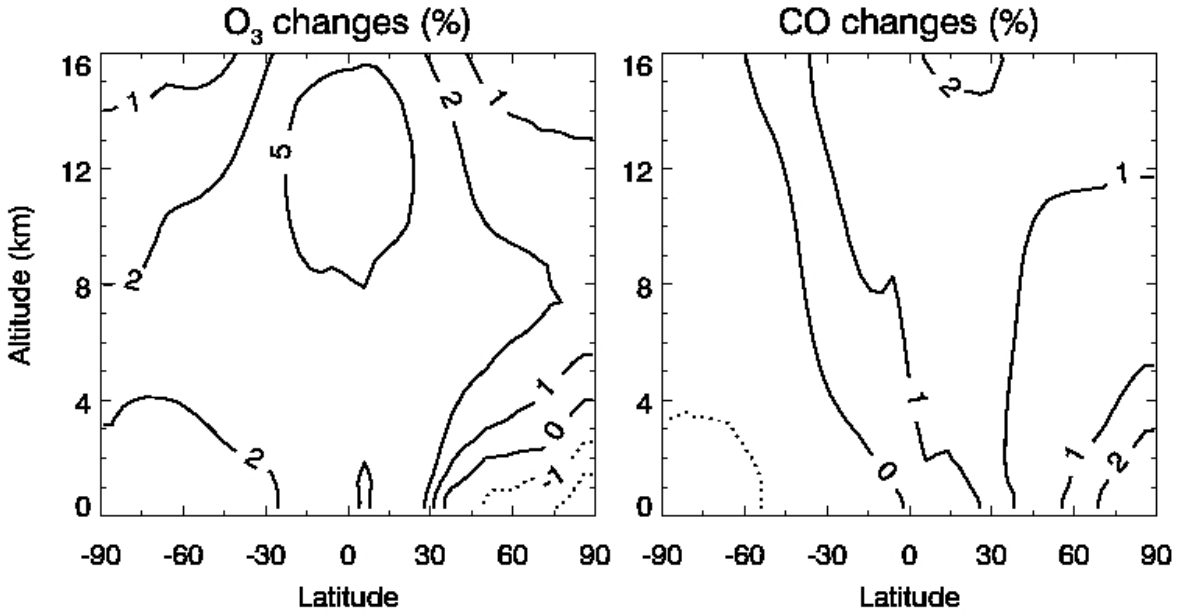

Figure 11. Simulated percentage changes in monthly zonal mean (a) O_3 and (b) CO concentrations due to the radiative effect of clouds with the maximum-random cloud overlap assumption for June 2001.

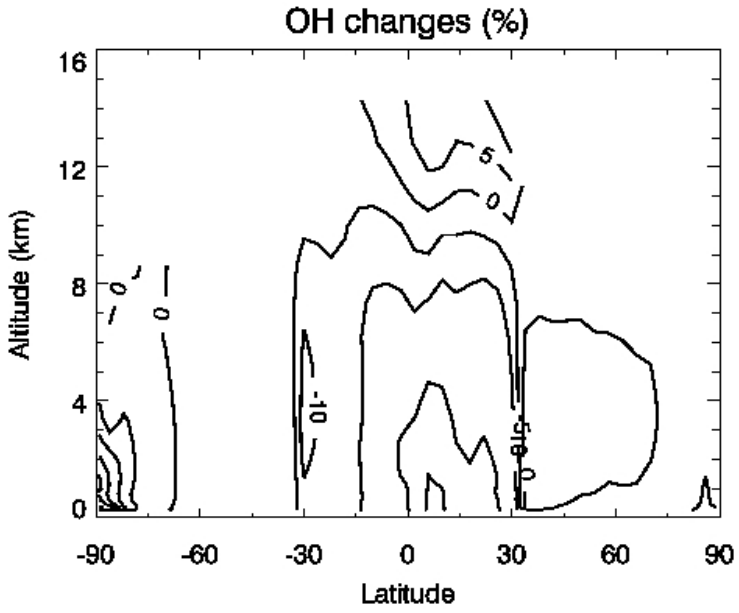

Figure 12. Simulated percentage changes in monthly zonal mean OH concentrations due to the radiative effect of tropical mid- and high- clouds (30^{o}S-30^{o}N) for June 2001, as reflected by subtraction of the simulation without tropical mid- and high- clouds from the simulation with global clouds. The linear assumption (LIN) is used.